

**ASSESSING THE USE OF RICE HUSKS AND SPENT GRAIN FOR THE
REMOVAL OF HEAVY METALS FROM SURFACE WATER**

JEREMIAH RICHARD KAYONGO

S21B32/129

**A FINAL YEAR RESEARCH AND DESIGN PROJECT REPORT SUBMITTED TO THE
FACULTY OF ENGINEERING, DESIGN AND TECHNOLOGY, IN PARTIAL FULFILLMENT
OF THE REQUIREMENTS FOR THE AWARD OF A DEGREE OF BACHELOR OF SCIENCE
IN CIVIL AND ENVIRONMENTAL ENGINEERING OF UGANDA CHRISTIAN UNIVERSITY**

April, 2025



**UGANDA CHRISTIAN
UNIVERSITY**

A Centre of Excellence in the Heart of Africa

ABSTRACT

This study assessed the use of rice husks and brewer's spent grain as adsorbents for removing heavy metals from River Nyamwamba's water. The research aimed to address the significant heavy metal contamination in the river, posing risks for domestic use. The study employed in-situ measurements of physico-chemical properties and heavy metal analysis, followed by laboratory experiments to determine the adsorption efficiency of the biochars of rice husks and brewers' spent grain. The findings revealed that a mix ratio of 1:3 (rice husks to brewer's spent grain) provided the most efficient removal of copper and iron, with removal efficiencies of 95.63% and 94.63%, respectively. The study concluded that steam activation significantly enhanced the adsorbents' performance, making them effective for improving water quality. These results highlight the potential of using agricultural by-products as sustainable and cost-effective solutions for water treatment in regions affected by heavy metal pollution.

DECLARATION

I KAYONGO RICHARD JEREMIAH with the following registration number **S21B32/129**, hereby declare that this is my original work, is not plagiarised and has not been submitted to any other institution for any award.

KAYONGO RICHARD JEREMIAH

S21B32/129

Signature:.....

Date:.....

APPROVAL

I certify that this report is for **KAYONGO RICHARD JEREMIAH, S21B32/129.** I fully accept that he has been under supervision and this research report can be submitted to the Department of Engineering, Design and Technology in partial fulfilment of a Bachelor of Science in Civil and Environmental Engineering of Uganda Christian University.

Mrs. Kyomukama Emma Immaculate

Academic Supervisor (Uganda Christian University)

Signature:.....

Date:.....

DEDICATION

To my beloved father and mother,

Your unwavering support, endless love, and boundless wisdom have been the guiding lights in my life. This work is a testament to your sacrifices, encouragement, and the values you instilled in me. I am forever grateful for your presence and the foundation you have provided.

ACKNOWLEDGEMENT

I would like to express my deepest gratitude to GOD for providing me with the strength, wisdom, and perseverance to complete this project.

I am profoundly grateful to my parents for their unwavering support, encouragement, and love throughout this journey.

My heartfelt thanks go to my supervisor, Mrs. Kyomukama Emma Immaculate, for her invaluable guidance, patience, and insightful feedback, which have been instrumental in the successful completion of this project.

I would also like to extend my sincere appreciation to my project partner, Ssebagala Sandra, for their collaboration, dedication, and hard work.

Lastly, I am thankful to the UCU lab technician, Mr. Ojara Eddy, for his technical assistance and support throughout the project.

TABLE OF CONTENTS

ABSTRACT	ii
DECLARATION	iii
APPROVAL	iv
DEDICATION	v
ACKNOWLEDGEMENT	vi
TABLE OF CONTENTS	vii
LIST OF TABLES	xiv
LIST OF FIGURES	xv
GLOSSARY OF TERMS AND ACRONYMS.....	xvii
CHAPTER ONE: INTRODUCTION	1
1.1 BACKGROUND	1
1.2 PROBLEM STATEMENT	2
1.3 MAIN OBJECTIVE	3
1.4 SPECIFIC OBJECTIVES	3
1.5 RESEARCH QUESTIONS	3
1.6 JUSTIFICATION	4
1.7 GEOGRAPHIC SCOPE.....	5
1.8 TIME SCOPE	6
CHAPTER TWO: LITERATURE REVIEW.....	7
2.1 Introduction	7

2.2 Water Quality	7
2.2.1 Physico-chemical qualities	7
2.2.1.1 Electrical Conductivity (EC)	7
2.2.1.2 Total Dissolved Solids (TDS).....	7
2.2.1.3 pH	8
2.2.2 Heavy metals.....	8
2.3 Materials	9
2.3.1 Rice husks as an adsorbent and preparation	9
2.3.2 BSG as an adsorbent and preparation	9
2.3.3 Activation of adsorbents	9
2.3.3.1 Types of Activation Techniques.....	10
2.3.3.1.1 Physical Activation	10
2.3.3.1.2 Chemical Activation.....	10
2.3.3.1.3 Combined Physical and Chemical Activation	11
2.4 Water Treatment	11
2.4.1 Conventional treatment methods in relation to adsorption	11
2.4.1.1 Chemical precipitation	11
2.4.1.2 Ion Exchange	11
2.4.1.3 Membrane Filtration	12
2.4.1.4 Chemical and Electrocoagulation	12
2.5 Adsorption	12

2.5.1 Types of Adsorption	13
2.5.1.1 Physical adsorption.....	13
2.5.1.2 Chemical Adsorption	13
2.5.2 Factors Affecting the Adsorption Process	14
2.5.2.1 Temperature	14
2.5.2.2 Nature and Surface Area of Adsorbent	14
2.5.2.3 pH of the Solution.....	14
2.5.2.4 Concentration of Adsorbate	14
2.5.2.5 Presence of Competing Substances	15
2.5.2.6 Ionic Strength of the Solution	15
2.5.2.7 Contact Time.....	15
2.5.3 Adsorbents.....	15
2.5.3.1 Types of Adsorbents	16
2.5.3.1.1 Carbon-based adsorbents	16
2.5.3.1.2 Zeolites	16
2.5.3.1.3 Metal-organic frameworks (MOFs)	16
2.5.3.1.4 Polymeric adsorbents.....	16
2.5.4 Adsorption Isotherms	17
2.5.4.1 The Langmuir isotherm.....	17
2.5.4.2 The Freundlich isotherm	18
2.5.5 Maximum Adsorption Capacity	20

2.5.6 Breakthrough Curves and Mass Transfer Zone	20
2.5.7 Adsorbent regeneration	20
2.5.7.1 Types of regeneration	21
2.5.7.1.1 Thermal Regeneration.....	21
2.5.7.1.2 Chemical Regeneration.....	21
2.5.7.1.3 Steam Regeneration	21
2.5.7.1.4 Electrochemical Regeneration	22
2.5.7.1.5 Biological Regeneration	22
CHAPTER THREE: METHODOLOGY	23
3.1 Introduction	23
3.1.1 Research Design	23
3.1.2 Area of Study.....	24
3.2 Determining the physico-chemical quality characteristics of the raw water from the river.	25
3.2.1 Materials and Equipment.....	25
3.2.2 Field Measurement Procedure	25
3.2.2.1 Site Selection and Sample Point Identification	25
3.2.2.2 Sampling procedure.....	26
3.2.2.3 Heavy metal ion measurement using the FAAS (APHA 3111 B).....	27
3.2.3 Post-Measurement Handling	27
3.2.4 Quality Control	27

3.2.5 Safety Considerations.....	28
3.3 Determining the sorption properties of rice husks and Brewer's spent grain.	
.....	29
3.3.1 Material preparation	29
3.3.1.1 Pyrolysis	29
3.3.1.2 Activation.....	29
3.3.2 FTIR Characterisation Procedure.....	29
3.4 Determining the optimum mixing ratios of rice husks and brewer's spent grain to remove heavy metals from the water.....	31
3.4.1 Materials and Equipment.....	31
3.4.2 Experimental Procedures.....	31
3.4.2.1 Column experiments to determine the Optimum Mix Ratio	31
3.4.2.2 Batch experiments to determine the Adsorption kinetics.....	32
3.4.2.3 Column experiments to determine the Optimum mix ratio.....	33
3.4.2.4 Column experiments to determine the Breakthrough characteristics	
.....	33
3.5 Designing the appropriate adsorption system	34
CHAPTER FOUR: RESULTS AND DISCUSSION.....	35
4.1 Introduction	35
4.2 IN-SITU TESTS OF PHYSICO-CHEMICAL CHARACTERISTICS AND HEAVY METAL TEST ANALYSIS	36
4.2.1 pH.....	36

4.2.2 Electrical Conductivity (EC)	37
4.2.3 Total Dissolved Solids (TDS)	38
4.2.4 Heavy Metals (Copper and Iron).....	39
4.3 FOURIER TRANSFORMS INFRARED SPECRTOSCOPY	42
4.3.1 Brewers' Spent Grain	42
4.3.2 Rice Husks	43
4.4 LABORATORY EXPERIMENTS.....	44
4.4.1 Optimum mix ratio for RH and BSG	44
4.4.2 Removal Efficiency, R_{eff} and Adsorbent Phase Concentration, Q_e	45
4.4.3 Adsorption isotherms	46
4.4.3.1 Langmuir Adsorption isotherms	46
4.4.3.2 Freundlich Adsorption isotherms.....	48
4.4.4 Determining optimum mass and corresponding column height.....	50
4.4.5 Breakthrough curves	51
4.5 DESIGN OF THE ADSORPTION TANK.....	52
4.5.1 Small scale design	52
4.5.2 Large Scale Design	54
CHAPTER FIVE: CONCLUSIONS AND RECOMMENDATIONS.....	57
5.1 CONCLUSIONS	57
5.2 RECOMMENDATIONS	58
REFERENCES	60

APPENDICES.....	74
APPENDIX A: TABLES OF RESULTS	74
APPENDIX B: PICTORIAL	77
APPENDIX C: CERTIFICATES OF ANALYSIS	81

LIST OF TABLES

Table 1: Summary of results.....	35
Table 2: Results for the Langmuir Isotherm for copper	46
Table 3: Results for the Langmuir Isotherm for iron	47
Table 4: Results for the Freundlich Isotherm for copper.....	48
Table 5: Results for the Freundlich Isotherm for iron	49
Table 6: Summary of Random packed column dimensions.....	52
Table 7: Results from variation of different mix ratios of adsorbents in column experiment	74
Table 8: Results from variation of mass of adsorbent at 150rpm for 90 minutes contact time.....	74
Table 9: Results from the varying column masses and corresponding heights	75
Table 10: Results from the breakthrough curves experiment	76

LIST OF FIGURES

Figure 1: Research Design Flow Chart	23
Figure 2: Map showing area of study.....	24
Figure 3: pH in situ results	36
Figure 4: Electrical Conductivity in situ results	37
Figure 5: Total Dissolved Solids in situ results	38
Figure 6: Iron in situ results.....	39
Figure 7: Copper in situ results	39
Figure 8: Brewers' Spent Grain FTIR graph.....	42
Figure 9: Rice Husk FTIR graph	43
Figure 10: Average Removal efficiency against varying mix ratios	44
Figure 11: Removal Efficiency against varying masses	45
Figure 12: Copper Langmuir Isotherm Graph	46
Figure 13: Iron Langmuir Isotherm Graph	47
Figure 14: Copper Freundlich Isotherm Graph.....	48
Figure 15: Iron Freundlich Isotherm Graph	49
Figure 16: Optimum removal efficiency for varying masses.....	50
Figure 17: Breakthrough curves graph for copper and iron.....	51
Figure 18: Sediment sampling	77
Figure 19: Water column sampling	77
Figure 20: Residents washing from river	77
Figure 21: In situ testing with multimeter	77
Figure 22: Sealed material in pots	78
Figure 23: Activated BSG and RH	78
Figure 24: Sieving materials.....	78

Figure 25: Material mass ratios	78
Figure 26: Batch experiment set up	79
Figure 27: Analytical Reagents.....	79
Figure 28: Setting up column bed	79
Figure 29: Filtering samples.....	79
Figure 30: Laboratory setup.....	80
Figure 31: Prototype setup	80

GLOSSARY OF TERMS AND ACRONYMS

Acronym/ symbol	Full form
APHA	American Public Health Association
BSG	Brewers' Spent Grain
Cu	Copper
EC	Electrical Conductivity
FAAS	Flame Atomic Absorption Spectroscopy
Fe	Iron
FTIR	Fourier Transforms Infrared Spectroscopy
HM	Heavy Metal
ISO	International Organisation for Standardisation
kg	kilogram
mg/L	milligrams per litre
ppm	parts per million
RH	Rice Husk
SEM	Scanning Electron Microscopy
TDS	Total Dissolved Solids
US:EAS	Uganda Standard
WHO	World Health Organisation
$\mu\text{S}/\text{cm}$	micro-Siemens per centimetre

CHAPTER ONE: INTRODUCTION

1.1 BACKGROUND

The Kasese district is centred in Kilembe, an old mining town at the foot of the Rwenzori Mountains. Alongside the Nyamwamba River, it is home to the legendary Kilembe Mines, a copper and cobalt mining company established in colonial Uganda. Kilembe Mines' rusty and dilapidated facilities, which dominate the skyline, are easily seen against the surrounding vegetation (Masereka et al. 2022).

After being established as a mining company in the 1950s, Kilembe Mines produced and exported copper until the late 1970s. These mines were once operated by Falcon-bridge, but the pounds of leftover copper tailings pose a major environmental risk today. Due to their erosion into the river, these dangerous tailings have contaminated the land and water sources (Mwesigye and Lawrence, 2022).

According to Amjad et al., (2020), for living things, drinking and irrigation water contaminated with heavy metals (Cr, Cd, Hg, As, Zn, Cu, Fe, Al, Ba, Ca, Mg, Pb, Mn, Ag, Na, and Se) in excess or below what the body needs is extremely harmful. Many sectors, including mining, textiles, leather, insecticides, plastic, wood, and medicines, are their main suppliers. These metals are released into the air, surface water, soil, groundwater, and crops by industrial operations, and they eventually endanger human health. Anthropogenic activities such as the discharge of petroleum, oil, road salts, mining, fertilisers, pesticides, and other man-made materials into groundwater can contaminate it.

1.2 PROBLEM STATEMENT

The second most important element for human life is drinking water; without it, life cannot exist. Nevertheless, it is currently difficult to find pure water for human use, and the remaining 3% of freshwater is heavily polluted globally (Amjad et al, 2020). According to Mwesigye and Lawrence (2022), mining operations in Kilembe concluded in 1978; however, the extraction and processing of copper in Western Uganda resulted in significant deposits of cupriferous and cobaltiferous pyrites within the mountain river valley, accompanied by mine water which is channelled to the surface.

Masereka et al. (2022) conducted research revealing significant heavy metal contamination in the Nyamwamba River. The concentrations of heavy metals in the raw water, including Iron (Fe) at **10.21 mg/L** and Copper (Cu) at **5.29 mg/L**, exceed the Uganda Standards for potable water guideline values of **0.3 mg/L** and **1.0 mg/L**, respectively, posing risks for domestic and agricultural use by residents. This research also indicated higher levels of the heavy metal contamination in the wet season as compared to the dry season. Agriculturists cultivating near the Nyamwamba River in the Kasese district of Western Uganda observe that their crops wither whenever the riverbanks inundate, and the district's rising incidence of cancer and ulcers is anecdotally ascribed to the ingestion of contaminated water from supplies polluted by Kilembe copper mine tailings (Masereka et al., 2022).

This research study is therefore aimed at assessing the use of rice husks and brewer's spent grain as adsorbents for the removal of heavy metals ions from the raw water of river Nyamwamba that can be employed by the community for domestic use.

1.3 MAIN OBJECTIVE

To assess the use of Rice Husks and Brewer's Spent Grain as adsorbents for the removal of heavy metals from the raw water of river Nyamwamba.

1.4 SPECIFIC OBJECTIVES

1. To determine the physico-chemical quality characteristics of the raw water from the river.
2. To determine the sorption properties of rice husks and brewer's spent grain.
3. To determine the optimum mixing ratios of rice husks and brewer's spent grain to reduce heavy metals from the water.
4. To design an appropriate treatment system.

1.5 RESEARCH QUESTIONS

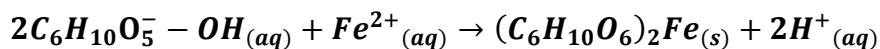
1. What is the heavy metal concentration in the water of River Nyamwamba?
2. What are the sorption properties of rice husks and brewer's spent grain?
3. What are the optimum mixing ratios of rice husks and brewer's spent grain to remove heavy metals from the water?
4. What are the appropriate dimensions for the effective functioning of the treatment system?

1.6 JUSTIFICATION

Due to its high cellulose and lignin content, brewer's spent grain (BSG) is a substance that shows promise for heavy metal adsorption from water. Functional groups like hydroxyl ($-OH$) and carboxyl ($-COOH$) in cellulose provide binding sites that enable coordination with heavy metal ions (Wierzba and Klos, 2019).

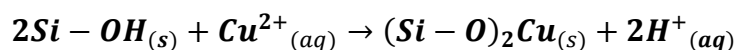
Because of their higher charge density and smaller ionic radii, metals like iron (Fe^{2+}) and lead (Pb^{2+}) are more likely to form stable complexes with negatively charged carboxylate groups. Strong metal binding results from the hydroxyl groups in BSG forming stable inner-sphere complexes with metals (Wierzba and Klos, 2019).

The adsorption of iron on BSG biochar, for instance, can be explained as follows:



Due to their special qualities, rice husks have a synergistic impact that improves the performance of heavy metal adsorption when added to brewer's spent grain (BSG). Silica is abundant in rice husks. For example, silanol groups exhibit greater affinity for metals such as zinc (Zn^{2+}) and copper (Cu^{2+}) since they pose a low charge densities and larger ionic radii. These metals frequently form outer-sphere complexes where the electrostatic attraction between the negatively charged silanol groups and the metal cations plays a more significant role in the interaction than covalent bonding as is the case with the carboxyl groups (Priya et al., 2022).

The adsorption of copper on rice husk biochar, for instance, can be explained as follows:



Additionally, the biochars of these bio adsorbents have the potential to be regenerated using chemical desorption whereby acids, bases or salts can be applied to detach heavy metal ions from the surfaces and pores of the adsorbents. This can be done for about 4-10 cycles before significant loss of adsorption efficiency of the biochars settles in (Velempini et al., 2023).

The rice husks will be obtained from Mubuku Irrigation Scheme milling plant located in Mubuku whereas the Brewer's spent grain shall be obtained from Nile Breweries Mbarara Branch located in Mbarara.

Due to Uganda's high rate of alcohol consumption and the fact that breweries are always operating, BSG is easily accessible throughout the year. It is estimated that 85% of the by-products from beer brewing contain BSG, with 20 kilogrammes of BSG produced for every 100 litres of alcohol produced (Kabirizi and Kato, 2023). Since the Nile Breweries Limited Mbarara Plant, where BSG is to be obtained, generates 1.3 million hectolitres per year, roughly 26 million kilogrammes of BSG are generated annually (NBL, 2024).

In addition to that due to the Mubuku Irrigation Scheme, which has over 80 hectares of land set aside for rice cultivation and yields an average of 2.5 tonnes per hectare per agricultural year, rice husks are also easily accessible in Kasese district (Wanyama et al., 2024).

1.7 GEOGRAPHIC SCOPE

Nyamwamba River is located in Kasese district in the western part of Uganda (0012'30.0" N, 30000'25.0" E). It is the main river of the Rwenzori Mountains and is fed by melting glaciers from the mountains of the moon. The river emerges from

Rwenzori Mountain and flows to Lake George in the Albertine Rift, stretching an estimated distance of 126 km.

The specific region of interest is Nyakasanga I parish located at the extremes of Kasese district about 800m from the Nyamwamba River where residents depend on the surface water for domestic and agricultural purposes.

1.8 TIME SCOPE

This research study was carried out from the month of October, 2024 to the month of April, 2025.

CHAPTER TWO: LITERATURE REVIEW

2.1 Introduction

This section reviews existing studies on water quality and treatment methods with a focus on physico-chemical parameters like electrical conductivity (EC), total dissolved solids (TDS), and pH. These are key indicators of heavy metal contamination. It also explores the environmental and health impacts of heavy metals in raw water. This review also looks at bio adsorbents like rice husks (RH) and brewer's spent grain (BSG) alongside conventional treatment methods and the various preparation techniques. The findings help in understanding current water treatment technologies and how they can be improved.

2.2 Water Quality

2.2.1 Physico-chemical qualities

2.2.1.1 Electrical Conductivity (EC)

Electrical Conductivity indicates the level of dissolved ions in water. Elevated EC levels generally indicate a high metal pollution due to the dissolved ions. Elevated EC values also affect adsorption by causing ionic competition which can inhibit heavy metal binding onto adsorbents. For example, in multi-metal solutions, metals with greater ionic radii or valences can occupy adsorption sites (Kerketta et al., 2013).

2.2.1.2 Total Dissolved Solids (TDS)

TDS measures the overall concentration of dissolved solids including organic compounds and heavy metals like iron and copper. Elevated TDS levels suggest water contamination often from industrial and mining activities. Godson Ebenezer Adjobu et al., (2023) demonstrates that adsorption efficiency tends to decrease in high-TDS

water due to competition among ions necessitating pre-treatment to lower TDS and improve metal removal.

2.2.1.3 pH

pH directly influences heavy metal solubility, ion speciation, and adsorbent surface charge. Under acidic conditions, metals remain in dissolved ionic states (e.g., Cu²⁺, Fe²⁺), favouring adsorption. However, extreme pH levels can degrade adsorbent material or lead to metal precipitation, reducing adsorption efficiency. Optimization of pH is critical for achieving high removal rates in adsorption systems (Li et al., 2013).

2.2.2 Heavy metals

Heavy metals are generally defined as metallic elements with high densities, atomic weights, or atomic numbers, typically above 5 g/cm³ (Tchounwou et al., 2012). Their definition can vary slightly depending on the context, but they are often characterized by their toxicity, persistence in the environment, and potential to bio accumulate in living organisms (Järup, 2003).

Heavy metals are introduced into surface waters through natural processes such as weathering of rocks and volcanic activity, as well as through anthropogenic activities like mining, industrial effluents, agricultural runoff, and improper waste disposal (Singh et al., 2011). Once present in aquatic ecosystems, these metals do not degrade, leading to their accumulation in sediments and potential uptake by aquatic organisms, posing serious risks to both environmental and human health (Alloway, 2013).

2.3 Materials

2.3.1 Rice husks as an adsorbent and preparation

Rice husks are a renewable agricultural by-product rich in silica, cellulose, and hemicellulose. Their abundant hydroxyl (-OH) and silanol (Si-OH) groups make them effective for heavy metal adsorption. Various pre-treatment processes, such as thermal activation (e.g., carbonization at 600°C), chemical modification (e.g., acid treatment with HCl or H₂SO₄), and functionalization with nanoparticles, enhance their adsorption capacity. Rice husks rich in silica have showed removal efficiency exceeding 90% for lead (Pb²⁺) and cadmium (Cd²⁺) (Chen et al., 2019).

2.3.2 BSG as an adsorbent and preparation

Brewer's spent grain (BSG) is a brewing residue made up of cellulose, hemicellulose, lignin, and protein. Because of its porous structure and presence of carboxyl (-COOH) and hydroxyl (-OH) functional groups, it possesses the excellent property of having the ability to uptake heavy metals such as chromium (Cr⁶⁺), zinc (Zn²⁺), and nickel (Ni²⁺) efficiently. Pre-treatment methods such as acid washing, enzymatic hydrolysis, and carbonization enhance adsorption efficiency by expanding the surface area and revealing more binding sites. In recent studies, blending BSG with other materials has also been investigated in a bid to further enhance its performance (Pereira et al., 2024).

2.3.3 Activation of adsorbents

Activation is the process of enhancing the porosity and surface area of pyrolysed carbonaceous materials to create activated carbon with superior adsorption properties. This process removes volatile compounds and develops a highly porous

structure, increasing the material's ability to capture adsorbates (Somi Doja, Lava Kumar Pillari and Bichler, 2021). It can be achieved using a wide variety of methods, all of which impact the final characteristics of the activated carbon, including the pore size distribution, surface characteristics, and capacity for adsorption. Which activation route to use depends on the intended application as well as the precursor used in the pyrolysis (Mehdi et al., 2022).

2.3.3.1 Types of Activation Techniques

2.3.3.1.1 Physical Activation

Physical activation is when materials that have already been pyrolysed are treated with oxidising agents like steam, carbon dioxide or air at high temperatures ranging from 600°C to 1200°C . This process helps to remove leftover tars and also helps form small pores in the carbon structure. Steam activation is commonly used for making activated carbon from coconut shells and wood because it creates a good pore structure (Panwar and Panwar, 2020).

2.3.3.1.2 Chemical Activation

Chemical activation is done by treating the raw material with certain chemicals like phosphoric acid (H_3PO_4), potassium hydroxide (KOH), or zinc chloride (ZnCl_2) before heating it to make carbon (Sakhiya et al., 2021). This method uses lower temperatures between 400°C and 800°C compared to physical activation but still results in activated carbon with many pores. Phosphoric acid is mostly used with raw materials such as wood and farm waste, while potassium hydroxide is preferred when making activated carbon with very small pores especially for things like super capacitors (Illingworth, Rand and Williams, 2022).

2.3.3.1.3 Combined Physical and Chemical Activation

Wiśniewska et al. (2022) mention that sometimes both chemical and physical methods are used together to improve the surface area and pore structure of activated carbon. This is usually done by first soaking the materials in chemicals and then heating it at high temperatures in an oxidising environment. This method is used for making high-performance carbon materials that are used in things like energy storage and gas adsorption, where having more surface area and specific pore size is important.

2.4 Water Treatment

2.4.1 Conventional treatment methods in relation to adsorption

2.4.1.1 Chemical precipitation

Chemical precipitation is accomplished through the addition of chemicals such as lime, alum, or ferric salts to precipitate out dissolved heavy metals as solid particulate matter. Lime precipitation, for instance, is suitable for the removal of metals such as copper and zinc but generates enormous quantities of sludge. Recent developments in co-precipitation methods, where heavy metals are co-precipitated along with other contaminants, have improved efficiency and lowered the sludge generation footprint (Siddha & Kumar, 2024).

2.4.1.2 Ion Exchange

Ion exchange/ resins are used to selectively remove heavy metal ions from water by exchanging them with harmless ions like Na^+ or H^+ . Modern ion exchange systems

utilize chelating resins with higher specificity for metals such as lead, mercury, and cadmium. However, challenges like resin fouling and high costs for resin regeneration limit their large-scale application. Emerging nano-enhanced resins and magnetic ion exchangers aim to address these limitations by improving selectivity and operational durability (Bettine, 2023).

2.4.1.3 Membrane Filtration

Membrane filtration techniques, including ultrafiltration, nanofiltration, and reverse osmosis, remove heavy metals based on molecular size and charge. These methods achieve high removal rates for metals like arsenic (As^{5+}) and chromium (Cr^{6+}). Innovations in membrane materials, such as graphene oxide coatings and polymer composites, enhance filtration efficiency and resistance to fouling. Hybrid systems that integrate adsorption and membrane filtration are being explored to optimize water treatment performance (Li & Hausladen, 2023).

2.4.1.4 Chemical and Electrocoagulation

Chemical coagulation makes use of reagents like ferric chloride and alum, which function by neutralizing the charges of metal ions and thereby forming readily removable flocs. Electrocoagulation, however, employs electric currents to sacrifice anodes like aluminium or iron to form coagulants in the point of use. Both are highly effective in treating a broad spectrum of metals like arsenic, copper, and lead. Current advancements are aimed at making energy efficiency improvements, merging these techniques with adsorption to drive increased contaminant removal while simultaneously lowering chemical consumption (Bettine, 2023).

2.5 Adsorption

Adsorption is the process by which molecules, atoms or ions from a gas liquid or dissolved solid accumulate on the surface of a material rather than diffusing into it. It is a surface phenomenon driven by intermolecular forces like van der Waals interactions or chemical bonding (Lima et al., 2021). Unlike absorption where a substance is taken up by the entire volume of another material adsorption happens only at the interface between two phases. This process is widely used in industries such as water purification catalysis and gas separation. It can be classified into physisorption which involves weak physical forces and chemi-sorption which involves stronger chemical bonds (Topare and Wadgaonkar, 2022).

2.5.1 Types of Adsorption

2.5.1.1 Physical adsorption

Physical adsorption, also known as physisorption, happens when weak Van der Waals forces hold the adsorbate to the adsorbent. This process can be reversed and usually occurs at low temperatures (Lei et al., 2022).

2.5.1.2 Chemical Adsorption

Chemical adsorption, or chemisorption, occurs when strong bonds like covalent or ionic bonds are formed. This type is usually not reversible and happens at higher temperatures, often creating a single layer on the adsorbent's surface. (Sabadash and Lysko, 2023).

2.5.2 Factors Affecting the Adsorption Process

2.5.2.1 Temperature

Temperature is very important in adsorption. In physical adsorption, higher temperatures weaken the van der Waals forces, so less adsorption happens. In chemical adsorption, higher temperatures help the reaction and can increase adsorption (Morgan, Anstine and Colina, 2022).

2.5.2.2 Nature and Surface Area of Adsorbent

The physical and chemical properties of the adsorbent greatly impact adsorption efficiency. Adsorbents with a higher surface area to volume ratio provide more active sites for adsorption to occur. Additionally, the chemical nature of the adsorbent such as functional groups determines its affinity for adsorbates.

2.5.2.3 pH of the Solution

The pH of the solution is important because it changes the ionization of both the adsorbent and adsorbate. This is especially true for ion-exchange adsorption, where pH changes can increase or decrease how well the adsorbate sticks (N'diaye et al., 2022).

2.5.2.4 Concentration of Adsorbate

A higher concentration of adsorbate usually leads to more adsorption, as there are more molecules available to stick. However, when all the sites are filled, the process reaches a limit (Bullen et al., 2021).

2.5.2.5 Presence of Competing Substances

In systems with more than one substance, different adsorbates may compete for the same sites. This competition can lower the efficiency of adsorption for the target substance. The adsorbent's preference determines which substance sticks better (Morgana Macena et al., 2025).

2.5.2.6 Ionic Strength of the Solution

In water, a high ionic strength can block the electrostatic forces between the adsorbent and adsorbate, lowering the efficiency. Sometimes, it can also help by compressing the electrical double layer and promoting particle clumping, which improves interactions (Hu et al., 2013).

2.5.2.7 Contact Time

The time the adsorbate is in contact with the adsorbent is very important. A short contact time may not allow complete adsorption, while a longer time can help reach equilibrium and maximize adsorption. The needed time depends on the adsorbent type, how fast adsorption happens, and other conditions (Zhao et al., 2014).

2.5.3 Adsorbents

Adsorbents are materials that help in the adsorption process. They can be natural, man-made, or modified materials. Common examples are activated carbon, silica gel, zeolites, and metal-organic frameworks (MOFs). Their effectiveness depends on factors like surface area, porosity, and chemical attraction to the adsorbate (Alaqarbeh, 2021).

2.5.3.1 Types of Adsorbents

2.5.3.1.1 Carbon-based adsorbents

Carbon-based adsorbents, such as activated carbon, have high surface areas and many pores. They work well to remove organic contaminants, heavy metals, and gases. They are used in water treatment, air purification, and chemical recovery (Mahesh et al., 2022).

2.5.3.1.2 Zeolites

Zeolites are crystalline aluminosilicates with clear pore structures. They work well for gas separation and water cleaning. Their ion-exchange ability lets them selectively remove ions, making them useful for softening hard water and removing heavy metals (Irannajad and Kamran Haghghi, 2020).

2.5.3.1.3 Metal-organic frameworks (MOFs)

MOFs are very porous materials with adjustable structures. They are good for gas storage, separation, and catalysis. Their large surface area and customizable pore sizes help them capture greenhouse gases and treat industrial waste (Moghadam, Chung and Snurr, 2024).

2.5.3.1.4 Polymeric adsorbents

Polymeric adsorbents are synthetic materials made to selectively remove certain contaminants. They are often used in medicine, drug delivery, and wastewater treatment. These materials can be modified with specific groups to better capture targeted pollutants (Moradi and Sharma, 2021).

2.5.4 Adsorption Isotherms

Adsorption isotherms show how adsorbates stick to adsorbents at a constant temperature. The Langmuir and Freundlich isotherms are the two most common models used to describe these interactions (Al-Ghouti and Da'ana, 2020).

2.5.4.1 The Langmuir isotherm

The Langmuir isotherm assumes monolayer adsorption on a homogeneous surface with no interactions between adsorbed molecules. It is based on the concept that all adsorption sites are energetically equivalent and that once a site is occupied, no further adsorption can occur at that location (Saad Alafnan et al., 2021).

The equation for the Langmuir isotherm is:

$$\frac{1}{Q_e} = \frac{1}{Q_{max}K_L} * \frac{1}{C_e} + \frac{1}{Q_{max}}$$

Where;

Q_e - amount of adsorbed adsorbate molecule per gram of Adsorbent (mg/g)

Q_{max} - capacity of the adsorbent monolayer (mg/g)

C_e - adsorbate equilibrium concentration (mg/L)

K_L - Langmuir Adsorption constant

The separation factor, R_L

$$R_L = \frac{1}{1 + K_L C_e}$$

The separation factor has the following values;

$R_L > 1$, unfavourable adsorption process (allows the adsorption process to occur, most desorption processes occur)

$R_L = 1$, linear adsorption process (depending on the amount adsorbed and the concentration adsorbed)

$R_L = 0$, Irreversible adsorption process (strong adsorption)

$0 < R_L < 1$, Favourable adsorption process (normal adsorption)

Plotting a graph of $\frac{1}{Q_e}$ against $\frac{1}{C_e}$

Parameters

$$\frac{1}{Q_{max}} = \text{intercept}$$

$$Q_{max} = \frac{1}{\text{intercept}}$$

$$K_L = \frac{1}{Q_{max} * \text{slope}}$$

This model is particularly useful for predicting the maximum adsorption capacity of an adsorbate onto an adsorbent (Rajahmundry et al., 2021).

2.5.4.2 The Freundlich isotherm

The Freundlich isotherm describes multilayer adsorption on heterogeneous surfaces with varying adsorption sites. It accounts for surface heterogeneity and the possibility of stronger interactions at certain sites (Kalam et al., 2021).

The equation for the Freundlich isotherm is:

$$\ln Q_e = \ln K_f + \frac{1}{n} \ln C_e$$

Where;

Q_e - amount of adsorbed adsorbate molecule per gram of adsorbent (mg/g)

C_e - adsorbate equilibrium concentration (mg/L)

K_F - adsorbate equilibrium concentration (mg/L)

n - value indicating degree of linearity between adsorbate solution and adsorption process

The value of n is described as follows;

$n = 1$, linear adsorption

$n < 1$, Adsorption process with chemical interaction

$n > 1$, adsorption process with physical interaction

Favourable adsorption process is declared when $0 < \frac{1}{n} < 1$, and a cooperative

adsorption process occurs when $\frac{1}{n} > 1$

Plotting a graph of $\ln Q_e$ against $\ln C_e$

Parameters

$\ln K_f = \text{intercept}$

$K_f = e^{\text{slope}}$

$\frac{1}{n_F} = \text{slope}$

$n_F = \frac{1}{\text{slope}}$

Unlike the Langmuir model, the Freundlich isotherm does not set a limit on how much can be adsorbed, which makes it better for adsorption processes that involve complex surfaces (Saad Alafnan et al., 2021).

2.5.5 Maximum Adsorption Capacity

Maximum adsorption capacity is the highest amount of adsorption an adsorbent can achieve under perfect conditions. This value is found using experimental data and mathematical models based on isotherm equations (Liu et al., 2024). Factors like the type of adsorbent, surface treatment, and environmental conditions affect this maximum capacity (Gayathiri et al., 2022).

2.5.6 Breakthrough Curves and Mass Transfer Zone

Breakthrough curves are graphs that show how the concentration of adsorbate in the output changes over time, which helps in checking how effective an adsorption column is (Apiratikul and Chu, 2021). The mass transfer zone (MTZ) is the area in the column where adsorption is happening most actively (Danish et al., 2022). A shorter MTZ means that the adsorption is more efficient, while a longer MTZ indicates that the adsorbent may not be used effectively and could lead to breakthrough (Danish et al., 2022). These measurements are very important when designing systems for separation and purification based on adsorption.

2.5.7 Adsorbent regeneration

Adsorption regeneration refers to the process of restoring an adsorbent's capacity by removing previously adsorbed substances, allowing the material to be reused.

Regeneration is essential in maintaining the efficiency and cost-effectiveness of adsorption-based systems, particularly for industrial applications where continuous operation is required (None Renu and Thandiwe Sithole, 2024).

2.5.7.1 Types of regeneration

2.5.7.1.1 Thermal Regeneration

Thermal regeneration involves heating the adsorbent to high temperatures to desorb the retained adsorbate. This method is widely used for carbon-based adsorbents such as activated carbon, where adsorbates with relatively low thermal stability can be effectively removed (P. Márquez et al., 2022). The high temperatures break intermolecular forces, allowing the adsorbate to evaporate or degrade. However, excessive heating may damage the adsorbent's structure, leading to reduced adsorption capacity over multiple cycles (Sonmez Baghirzade et al., 2021).

2.5.7.1.2 Chemical Regeneration

Alsawy et al. (2022) explain that chemical regeneration uses solvents, acids, or alkaline solutions to remove substances that have been adsorbed from the surface of the adsorbent. This method works well for ion-exchange resins and certain polymeric adsorbents. Changing the chemical environment causes the adsorbates to either dissolve or be pushed off, which restores the adsorbent's active sites. The type of chemical used depends on the nature of the adsorbate, and care must be taken to avoid causing permanent damage to the adsorbent.

2.5.7.1.3 Steam Regeneration

According to Jareteg et al. (2021), steam regeneration is an effective way to remove volatile organic compounds (VOCs) and other adsorbates from porous adsorbents like

activated carbon and zeolites. When steam is introduced, it pushes the adsorbates away by reducing their interaction with the adsorbent surface. This method is common in wastewater treatment and air purification because it is environmentally friendly and does not require harsh chemicals.

2.5.7.1.4 Electrochemical Regeneration

Electrochemical regeneration is a modern method that uses an electric current to help remove adsorbates. This technique is especially useful for adsorbents that remove heavy metals because it can selectively regenerate them by changing the oxidation state of the adsorbed species. It is highly efficient and produces very little secondary waste, making it a good option for sustainable wastewater treatment processes (Zhou et al., 2021).

2.5.7.1.5 Biological Regeneration

Biological regeneration uses microorganisms to break down or transform adsorbed substances into harmless by-products. This approach is often used for bio-based adsorbents and in activated sludge systems. The success of this method depends on factors such as the activity of the microorganisms, the nature of the adsorbate, and the surrounding environmental conditions (Jain et al., 2021).

CHAPTER THREE: METHODOLOGY

3.1 Introduction

This section explains the steps used to evaluate water quality and the effectiveness of biochar materials in removing heavy metals. It includes measuring the physical and chemical properties of river water, preparing and testing biochar made from rice husks and brewer's spent grain, and figuring out the best conditions for biochar-based water treatment, such as the proper mixing ratios, contact time, and pH. These steps are important because they provide useful data for creating effective water treatment solutions.

3.1.1 Research Design

A quantitative experimental design was used to evaluate the effectiveness of BSG and RH in removing heavy metals from water. Water samples were treated using different BSG-RH ratios in laboratory scale experiments. Parameters such as pH, Electrical Conductivity, Total Dissolved Solids, Iron and Copper were measured before and after treatment. Data were analysed to determine removal efficiency and compare treatment performance. Statistical analysis was used to validate the results. Below is the layout of the procedure followed to achieving the results from the experiments.

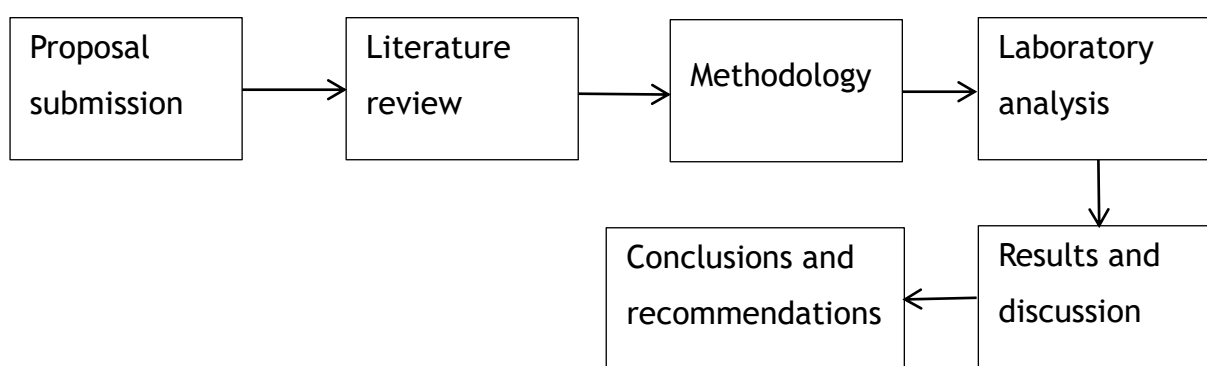


Figure 1: Research Design Flow Chart

3.1.2 Area of Study

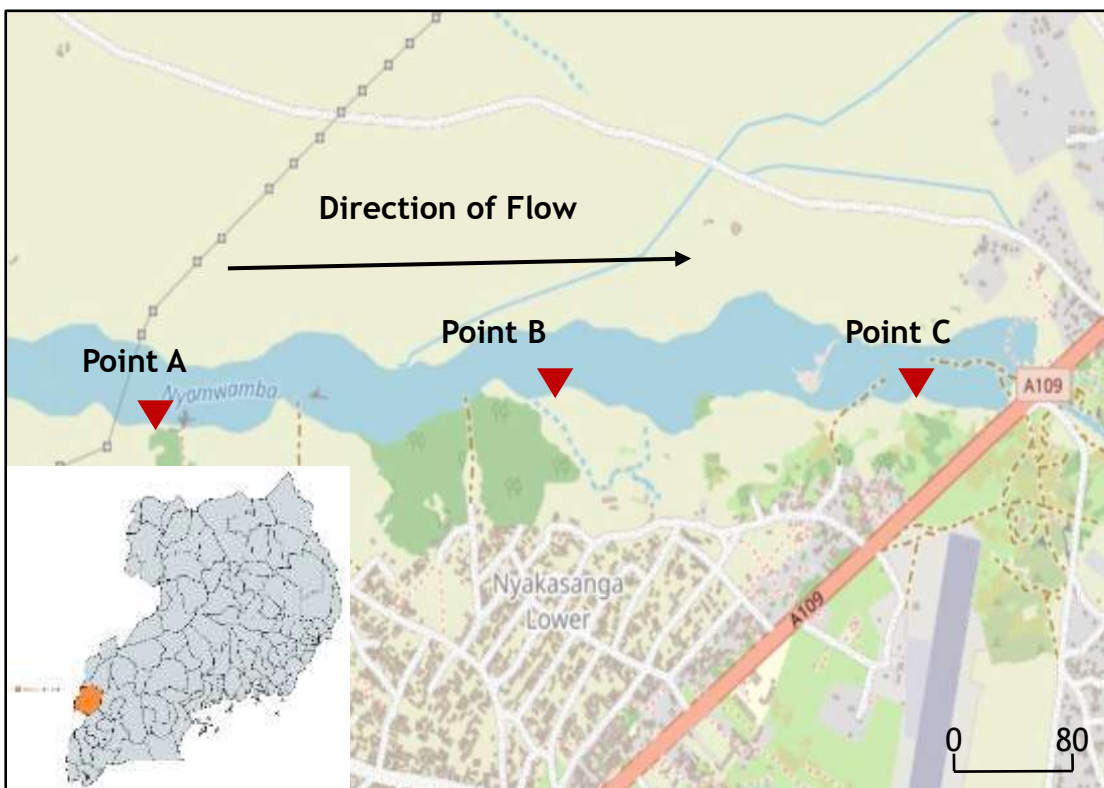


Figure 2: Map showing area of study

The study's focus is the Lower Nyakasanga I Parish region of the River Nyamwamba in Kasese district, Western Uganda ($00^{\circ}12'30.0''$ N, $30^{\circ}00'25.0''$ E), where the local population actively depends on the river as their sole supply of water for everyday household needs. Few individuals in this area can pay the National Water and Sewerage Corporation's (NWSC) treated water distribution, and the hilly terrain makes it difficult to deliver water to different homesteads (Oyesigye et al, 2024). The Kilembe mines with their enormous copper tailings dump along most of this section of the river in the upper section, domestic activities like washing motorbikes, bathing, and laundry in the mid-section, and sand/clay mining activity downstream are the main features of the Lower Nyakasanga region that was the focus of the study, as depicted on the map in *Figure 1*. With sample locations A ($0^{\circ} 11' 38''$ N, $30^{\circ} 4' 54''$ E) upstream, B ($0^{\circ} 11' 40''$ N, $30^{\circ} 5' 32''$ E) midstream, and C ($0^{\circ} 11'$

39°N, 30° 6' 6"E downstream, the sampling sections and points (A, B, and C) were chosen in accordance with the previously specified activities.

3.2 Determining the physico-chemical quality characteristics of the raw water from the river.

This procedure outlines the steps that were carried out for in situ measurement of pH, Electrical Conductivity (EC), and Total Dissolved Solids (TDS) in the river water using a multimeter. These measurements followed the guidelines specified in the APHA 23rd edition (2017).

3.2.1 Materials and Equipment

- i. Multimeter: A portable, calibrated device that was used to measure pH, EC, and TDS.
- ii. Distilled Water: Distilled water was used for rinsing probes between measurements.
- iii. Field Sampling Kit: The kit included gloves, sample containers, and data sheets.
- iv. Flame Atomic Absorption Spectrophotometer: This equipment was used to measure the concentration of the heavy metal ions in the raw water.

3.2.2 Field Measurement Procedure

3.2.2.1 Site Selection and Sample Point Identification

Sampling was done in the months of November 2024, December 2024 and January 2025. The water samples were picked from River Nyamwamba in Kasese district, Western Uganda (0012'30.0" N, 30000'25.0" E) focusing on Nyakasanga I Parish region where most of the population actively relies on the river as the only source of water for daily domestic use.

Three sampling points were selected along the section of the river namely A, B and C where three water samples and sediment samples were collected in the morning hours between **9am and 11am** with in -situ tests being done on pH, Electrical Conductivity, Total Dissolved Solids and Temperature for each sampling location. The sampling points were **5m** from the average river bank demarcations due to the seasonal changes of the river banks attributed to climate change.

3.2.2.2 Sampling procedure

The sampling procedure was determined according to World Health Organization and American Public Health Association standard guidelines for sampling for heavy metal analysis.

The borosilicate glass bottles for sample collection were first rinsed with the nitric acid 1:1 24 hours prior to sampling as a pre-conditioning method. This is done because samples collected were to be acidified (using nitric acid, 1:1 50%) in preservation of heavy metal ions (APHA, 2017).

During collection, the borosilicate glass was placed into the river at a subsurface depth of about 20cm with the mouth of the jar facing the water current of the river (upstream) till it was full. Nitric acid (1:1, 50%) was then added to the sample using glass droppers while taking note of the pH till the sample was at pH<2.

Afterwards the sample was labelled clearly indicating the details of sample number, location of sampling point, date, time, temperature and pH. The sample was then placed in a cooling box with ice to keep it in a temperature range of 4-8°C.

Simultaneously, in-situ tests for the other parameters pH, Electrical Conductivity (EC), Total Dissolved Solids (TDS) and Temperature were carried out three times at the location that the sample was picked using a multimeter. The multimeter probe was first rinsed with distilled water and then it was submerged into the sample ensuring that the sensor was fully covered. The values displayed on the screen of the multimeter were allowed to stabilize for 1-2 minutes before reading off and recording the values of the respective parameters.

3.2.2.3 Heavy metal ion measurement using the FAAS (APHA 3111 B)

The nitrified samples to be analysed for heavy metals of copper and iron were restored to their original in situ pH when collected. the sample containing the elements of interest was introduced into a flame and heated in a graphite furnace to atomise it then a monochromatic light source was then passed through this atomised sample. At the characteristic wavelength of the element being analysed, the atoms in the sample absorbed light. The amount of absorption is directly proportional to the concentration of the Heavy Metal ion concentration present in the sample. The concentrations of the ions were thus recorded.

3.2.3 Post-Measurement Handling

- i. The probe was rinsed and cleaned with distilled water after completing measurements.
- ii. The multimeter was stored according to the manufacturer's guidelines.

3.2.4 Quality Control

- i. Measurements were taken in triplicates at each sampling site to ensure reliability and accuracy of the measurements.

3.2.5 Safety Considerations

- i. Gloves were worn to prevent contamination and to protect against potential hazardous contact with the water.
- ii. Electrical components of the multimeter were kept dry and away from water.

3.3 Determining the sorption properties of rice husks and Brewer's spent grain.

3.3.1 Material preparation

3.3.1.1 Pyrolysis

The materials were collected and oven-dried at 105°C for 24 hours to remove moisture. The dried materials were loaded into pots with minimum compaction in order to allow for heat dissipation and sealed off. Thereafter they were subjected to slow pyrolysis by heating to a temperature of about 500°C in an oxygen limited environment for 3 hours to produce a biochar out of them. The biochar was allowed to cool in an inert environment to avoid oxidation.

3.3.1.2 Activation

After pyrolysis, the materials were both loaded into an autoclave and therefore subjected to steam of about 130°C for 2hours in order to activate these materials. Distilled water was used during this process and added when it was replenished.

3.3.2 FTIR Characterisation Procedure

The Fourier Transforms Infrared Spectroscopy (FTIR) analysis was used on the activated biochars in order to determine and identify the functional groups that were formed with each of these two materials before any treatment and after the activation treatment. The FTIR machine (model FT/IR-6600, Japan; M/C Serial Number No: - A027761790) was used in accordance to **ISO 10993-1 for Biomaterials**.

To rule out the presence of particles other than the samples being worked on, the background was first measured after turning on the machine without inserting any samples and a graph was plotted. After opening the machine and loading the sample onto the sample holder, the sensing lens was adjusted until it made slight contact

with the sample. Transmittance (%) Vs wavenumber (cm^{-1}) graphs were plotted and shown. Both the horizontal and vertical axes had scales set from 4000 to 400 cm^{-1} and 0 to 100%T respectively to provide key information about the functional groups present in the materials.

3.4 Determining the optimum mixing ratios of rice husks and brewer's spent grain to remove heavy metals from the water.

3.4.1 Materials and Equipment

- i. Biochars: Two types of biochar (Biochar A for Rice Husks and Biochar B for BSG) to be used.
- ii. Cotton: Cotton was used to act as a filtration bed at the bottom.
- iii. Sample Water: Surface raw water of known HM concentration or synthetic water with known heavy metal concentrations will be prepared.
- iv. A pH meter

3.4.2 Experimental Procedures

3.4.2.1 Column experiments to determine the Optimum Mix Ratio

A first column experiment was performed in order to ascertain the optimal mixing proportion of rice husk biochar (RH) and brewers spent grain biochar (BSG) as a single composite adsorbent material. Mixtures of the two biochars were prepared with different mass proportions of RH to BSG, along with controls of each biochar separately. The ratios used were of the following compositions; Only RH, 3:1(3 RH and 1 BSG), 1:1 (1 RH and 1 BSG), 1:3 (1 RH and 3 BSG) and Only BSG.

The column setup was made up of 6cm diameter containers (D1, D2, D3, D4, D5) which were each filled randomly with one of the mix ratios of the material and a thin layer of cotton at the bottom of the container as a support media for the adsorbent in the container.

A standard solution of 3mg/l copper and 3mg/l Iron was prepared in the laboratory from Copper (II) Sulphate Pentahydrate solution ($\text{CuSO}_4 \cdot 5\text{H}_2\text{O}$) and Iron (II) Sulphate

Heptahydrate solution ($\text{FeSO}_4 \cdot 7\text{H}_2\text{O}$) respectively. The solution was pH 7.0. This solution was allowed to pass through the various containers of different mix ratios of adsorbent above at a flow rate of 0.06 L/min left to flow by gravity and the filtrate collected from the bottom for each collected for analysis of heavy metals using the Flame Atomic Absorption Spectrometry (FAAS).

The mixture ratio that yielded the optimal average removal efficiency was ascertained and utilized as the optimal ratio and subsequently used in the rest of the experiments. The percentage removal efficiency was calculated from;

$$R_{eff} = \frac{(C_o - C_e)}{C_o} * 100$$

3.4.2.2 Batch experiments to determine the Adsorption kinetics

Batch tests were conducted in order to analyse the adsorption kinetics and the rate of consumption of the adsorbent with respect to the adsorbate. Different masses of the adsorbent were produced (5g, 10g, 15g, 15g, 20g, and 25g) by using the optimum mixing proportion (1:3 parts of RH to BSG). A known mass in each instance was added to a jar containing 500ml of the solution prepared by using 3mg/l concentration for copper and iron. The solution in every jar and its corresponding weight of the adsorbent was agitated at 150 revolutions per minute for 90 minutes. At the end of the 90 minutes, the solutions in every jar were filtered and the filtrates determined for heavy metals using FAAS.

The adsorbent phase concentration after equilibrium was determined for each mass variation was determined using;

$$Q_e = \frac{V}{M} * (C_o - C_e)$$

The adsorbent's maximum adsorption capacity was determined through the Langmuir and Freundlich adsorption isotherm models, and the acquired data were fitted to each model in order to identify the adsorption mechanism employed between the adsorbate and the adsorbent.

3.4.2.3 Column experiments to determine the Optimum mix ratio

Column experiments were carried out using different masses (40g, 60g and 80g) of the known mix ratio. These masses were each packed in a column with cotton at the bottom of the column as described before and a solution containing both the iron and copper at 3mg/L each was allowed to pass through the columns by gravity at flow rate of 0.06L/min. The filtrate at the bottom was collected and analysed for heavy metals using the FAAS. The optimum mass and corresponding height for the given parameters of flow rate and initial concentrations was then determined and used subsequently in the design to follow

3.4.2.4 Column experiments to determine the Breakthrough characteristics

The optimum mass obtained from the previous test was used to determine the breakthrough and exhaustion time of the material in the fixed bed column. A solution containing both concentrations of iron and copper 3mg/L each were passed through the material by gravity at a constant flow rate of 0.06 L/min. The experiment was left to run for a total of two hours and the at six different intervals, the concentrations were measured from filtrates obtained from the experiment. A graph of $\frac{C_o}{C_e}$ against time was plotted and the breakthrough time and exhaustion time of the materials were obtained when $\frac{C_o}{C_e} = 0.05$ and $\frac{C_o}{C_e} = 0.95$ respectively.

3.5 Designing the appropriate adsorption system

A granulated activated carbon (GAC) system was designed based on the demand capacity for a household in Nyakasanga parish following data from Uganda Water Supply Design Manual (MWE, 2013), World Health Organization (2020) and Uganda Bureau of Statistics (2024). The column adsorption system dimension specifications were calculated from the desired flow rate to cater for the daily household capacity, the adsorbent usage rate and the retention time of the system.

CHAPTER FOUR: RESULTS AND DISCUSSION

4.1 Introduction

This section of the report discusses the results obtained from the in-situ measurement of pH, Electrical Conductivity, Total Dissolved Solids and the heavy metal analysis of the preserved samples at each the respective sampling locations. It provides an insight into the possible reasons for why the respective values were obtained while adopting literature to back the possible reasons. There is further analysis that is done on the tests carried out on the material to determine of the activation procedure was achieved.

Table 1: Summary of results

PARAMETER	UNIT S	WET SEASON			DRY SEASON		
		A (n=3)	B (n=3)	C (n=3)	A (n=3)	B (n=3)	C (n=3)
pH		6.47	6.80	6.59	6.38	6.70	6.43
Electrical Conductivity (EC)	µS/c m	57.45±4. 52	61.30±9. 99	55.65±3. 12	49.70±4. 52	55.34±9. 99	52.30±3. 12
Total Dissolved Solids (TDS)	ppm	39.85±2. 00	43.60±5. 01	40.25±2. 76	37.34±2. 00	40.65±5. 01	39.00±2. 76
Iron, Fe	mg/L	2.763±0. 34	2.612±0. 46	2.323±0. 28	2.196±0. 34	1.908±0. 46	2.011±0. 28
Copper, Cu	mg/L	2.381±0. 78	1.798±0. 58	1.940±0. 55	1.372±0. 78	0.891±0. 58	1.028±0. 55

4.2 IN-SITU TESTS OF PHYSICO-CHEMICAL CHARACTERISTICS AND HEAVY METAL TEST ANALYSIS

4.2.1 pH

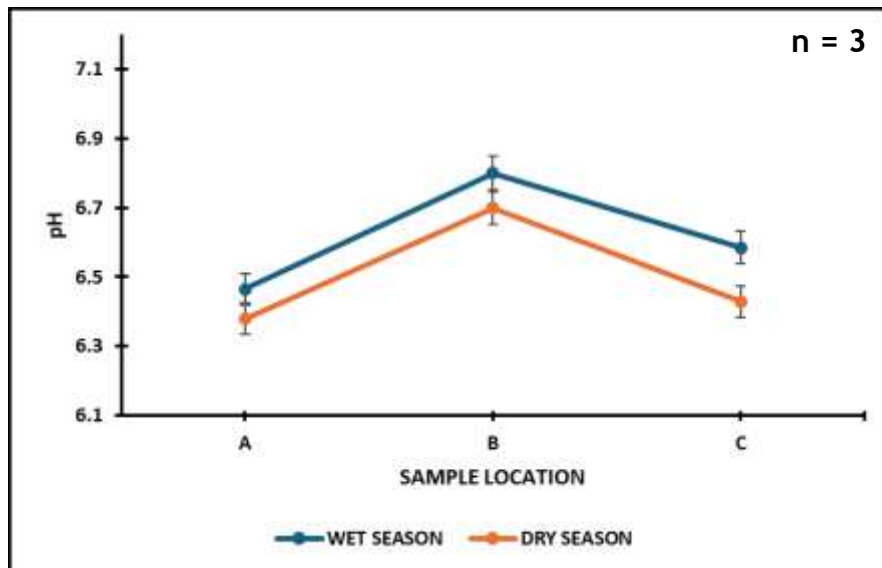


Figure 3: pH in situ results

The pH values across the sampling points ranged from 6.54 to 6.77. The Ugandan Standard for Natural Potable Water (US EAS 12:2014) recommends a pH range of 5.5-9.5, meaning the water at all points was within acceptable limits. Point A and point C were in the same pH range with slight increase of pH measured at point B.

At Point B, the pH increased compared to point A and point C, likely due to domestic activities such as laundry washing, bathing and motorcycle washing with which the detergents and soaps used tend to be alkaline. The general population was observed to discharge this domestic wastewater directly into the water way and some of these activities were carried out directly in the river continuously.

Studies have shown that contamination of wastewater from households particularly containing powdered detergents has led to an increase in the pH of streams (Goel and Kaur, 2012). Furthermore, detergents damage aquatic habitats, change the pH

balance, and interfere with microbes that control water quality, all of which lead to water pollution (Khan, 2022).

4.2.2 Electrical Conductivity (EC)

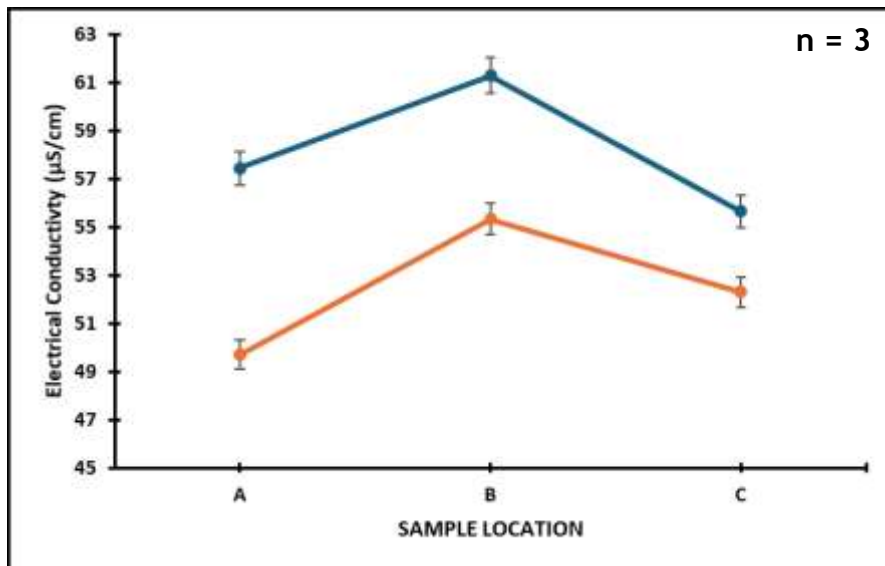


Figure 4: Electrical Conductivity *in situ* results

The average EC values across the three sampling sites range from 54.53 $\mu\text{S}/\text{cm}$ at Point C to 57.30 $\mu\text{S}/\text{cm}$ at Point B. Point A has a value of 54.87 $\mu\text{S}/\text{cm}$. These are all within the recommended standard of less than 1500 $\mu\text{S}/\text{cm}$, according to US EAS 12:2014.

At Point B, there is a small increase in EC, which might be caused by substances added to the river from household activities like washing. These substances can include nitrates and phosphates from laundry detergents and other domestic waste.

(Hardie et al., 2021) found that when greywater from homes, especially the kind that includes powdered detergents, is released into rivers, it raises the EC. This is because powdered detergents have high sodium and are more alkaline, which makes their EC higher than that of liquid detergents.

4.2.3 Total Dissolved Solids (TDS)

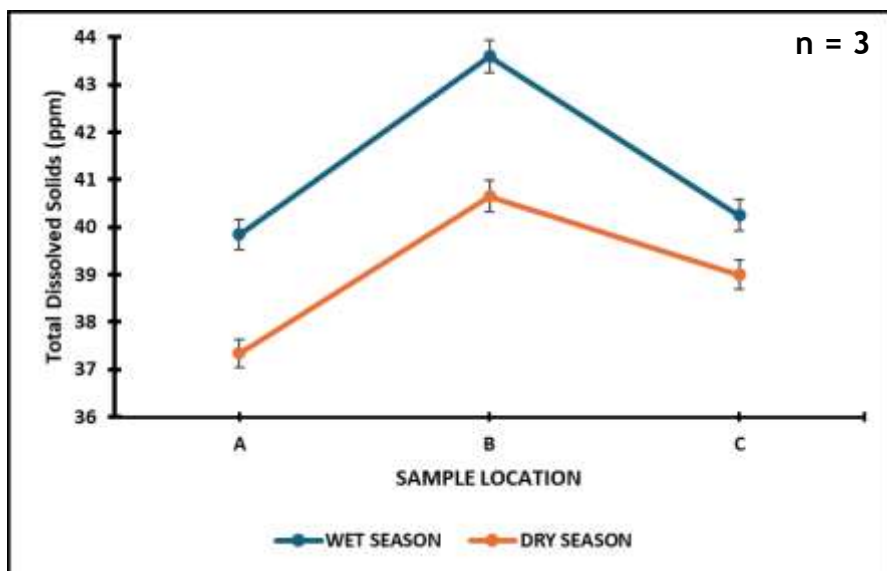


Figure 5: Total Dissolved Solids in situ results

The average TDS values are 38.70 mg/L at Point A, 41.53 mg/L at Point B, and 39.63 mg/L at Point C. These values are all much lower than the US EAS 12:2014 recommended limit of 1200 mg/L.

Just like EC, TDS also increases at Point B. This is probably because of the domestic wastewater that enters the river there. Wastewater from households contains detergents, organic matter, and oils, which all add dissolved and suspended particles, increasing the TDS.

When household greywater and powdered detergents introduce large concentrations of inorganic and organic matter, such as sodium carbonate, phosphates, and surfactants, the total dissolved solids (TDS) in river water rise. These substances stay dissolved in water, increasing TDS levels and changing the water's taste, purity, and aquatic life appropriateness. By dissolving into long-lasting chemical residues,

detergents add to the build-up of TDS and put additional strain on river ecosystems (Khan, 2022).

4.2.4 Heavy Metals (Copper and Iron)

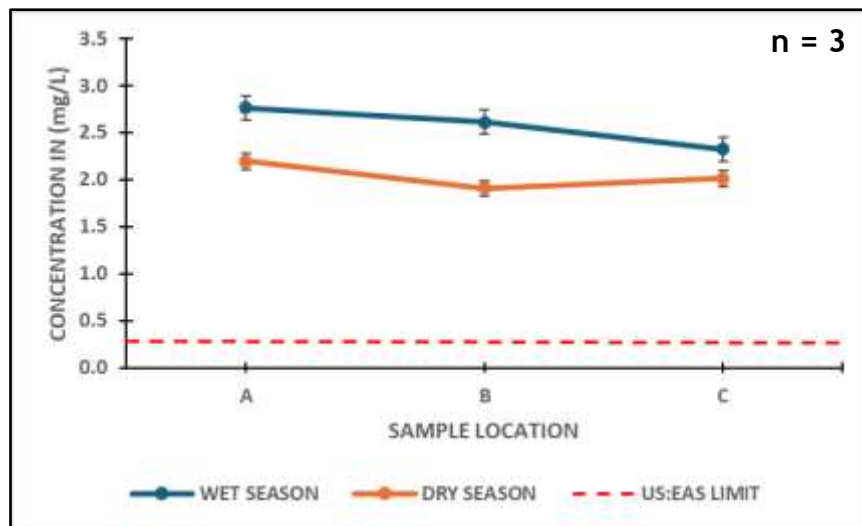


Figure 6: Iron in situ results

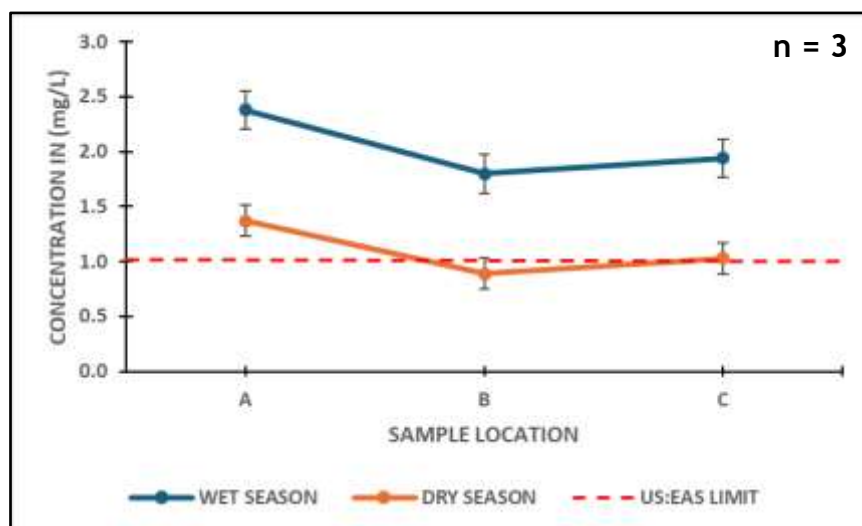


Figure 7: Copper in situ results

Copper and iron concentrations at all points exceed the US EAS 12:2014 Natural Potable water limits (1.0 mg/L for Cu, 0.3 mg/L for Fe) with copper ranging from 1.495 to 2.044 mg/L and iron ranging from 2.219 to 2.574 mg/L on average.

At Point A, the highest copper and iron concentrations were observed. Mineral tailings are the likely main source, as residual oxidation and slow weathering leading to leaching can continue to release heavy metal ions into the surrounding soils and subsequently into the river especially when there's a heavy downpour. At Point B, copper and iron levels decreased, likely due to metal adsorption onto organic matter from domestic water use containing detergents. At Point C, copper increased slightly, which may be attributed to sediment disturbance from mining activities in that region, while iron decreased due to precipitation and sedimentation.

Zhu et al. (2022) explained that mine tailings are one of the main sources of harmful metals. When exposed to the environment, they go through processes like weathering, oxidation, and leaching from rain. These metals can then move into nearby areas through wind, water seepage, and surface runoff. Precipitation is the most important factor in helping these metals move. According to Li et al. (2024), copper and other metals mostly move through surface water runoff.

Zhang et al. (2014) also found that when sediments are disturbed—either by things like floods or by animals digging—they can release heavy metals back into the water above. This is because disturbing the sediments changes how metals are shared between the water and the sediment. As a result, the metals can dissolve in the water and be taken in by aquatic life. This especially happens when the metals are stuck to fine particles in the sediment, which can be moved by flowing water once disturbed.

Atkinson et al. (2007) highlights that mining activities, particularly through excavation and runoff, can cause significant physical sediment disruption, leading to the remobilization of heavy metals. Disturbances in contaminated sediments alter

redox conditions, enhancing metal release into the water column. Similarly, Sadeghi et al, 2012 demonstrated that increased suspended sediment concentrations in runoff correlate with higher heavy metal content, emphasizing how mining-related erosion and sediment transport contribute to metal mobility.

Subsequently, it is also imperative to note that the trend was similar for both seasons however the wet season had generally higher concentrations of the heavy metals and this could be attributed to the increased leaching of metal concentrations into water due to rainfall events. This also holds for the remaining physico-chemical characteristics.

4.3 FOURIER TRANSFORMS INFRARED SPECTROSCOPY

4.3.1 Brewers' Spent Grain

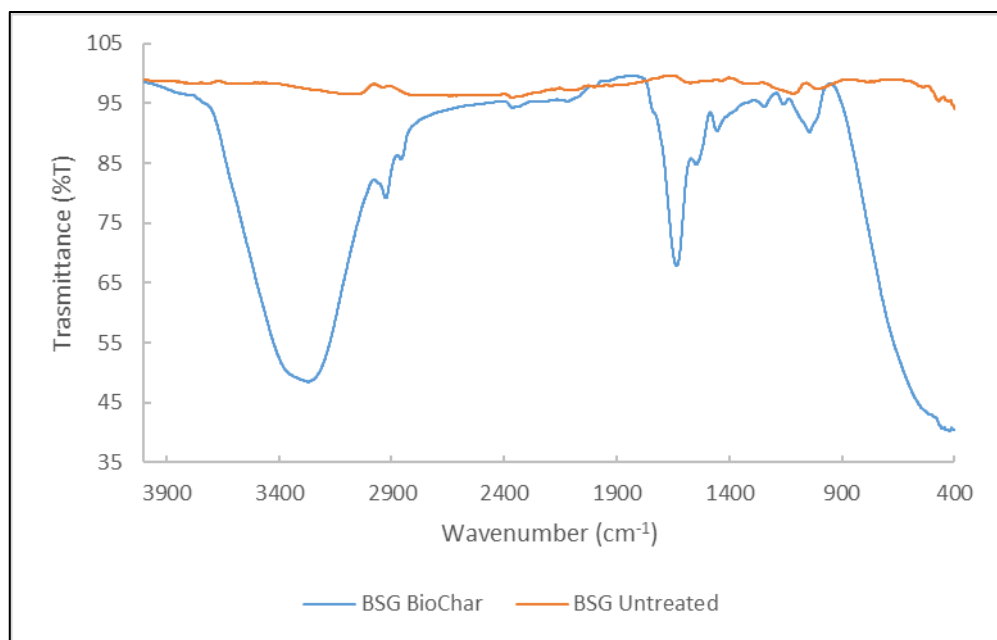


Figure 8: Brewers' Spent Grain FTIR graph

In the untreated Brewers' Spent Grain, no clear absorbance band was seen in the range that indicates a hydroxyl (-OH) group. However, after treatment, a broad absorbance band appeared between 3400 and 3200 cm⁻¹, which shows that a hydroxyl (-OH) stretching functional group is now present. This change is likely due to the steam treatment that was done on the Brewers' Spent Grain bio-char after pyrolysis to activate it.

Bardestani and Kaliaguine (2018) showed that steam activation can improve the surface chemistry of bio-char by increasing oxygen-containing functional groups like hydroxyl (-OH) groups. Their study on vacuum pyrolysis bio-char found that steam activation introduces functional groups that help improve adsorption properties. Mahmood et al. (2013) also looked at the pyrolysis and catalytic steam reforming of brewers' spent grain and confirmed that steam treatment after pyrolysis boosts

surface functionalities by increasing active oxygenated groups, including hydroxyl groups.

4.3.2 Rice Husks

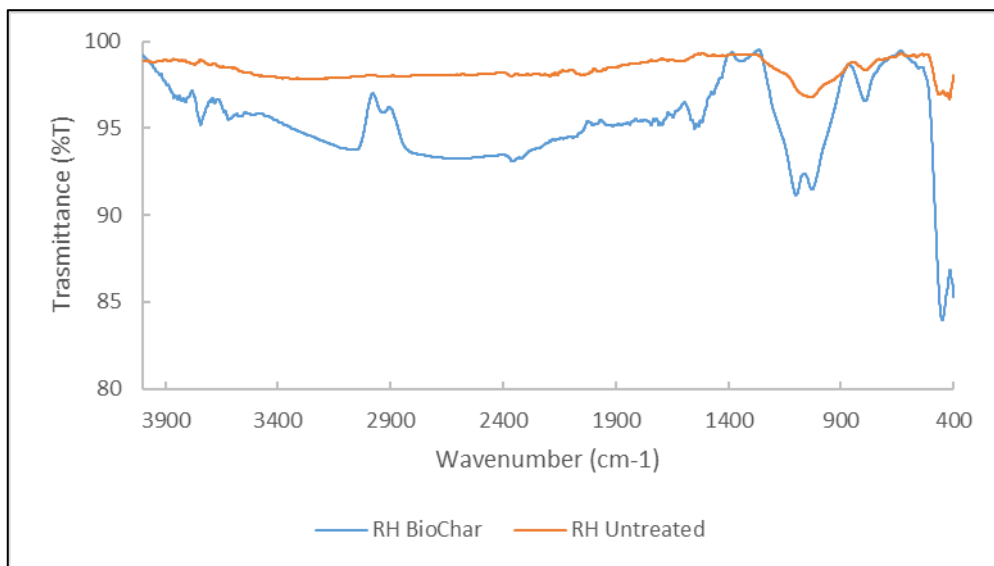


Figure 9: Rice Husk FTIR graph

Similarly, the untreated rice husks did not show a strong signal for silanol (-Si-OH) stretching groups in the normal range. After treatment, an absorbance band appeared between 1200 and 1000 cm⁻¹, indicating the presence of a silanol (-Si-OH) stretching functional group. This improvement in the functional group is likely due to the steam treatment done on the rice husk bio-char after pyrolysis to activate it.

Premchand et al. (2024) analysed the effects of activation and pyrolysis atmospheres on bio-char properties and discovered that activation, including steam treatment, significantly modifies surface functionalities, particularly silanol (-Si-OH) groups. Additionally, Zhang et al. (2021) discussed the role of functional bio-char design, emphasizing that activation processes, such as steam activation, enhance functional group formation, including silanol groups in silica-rich biomass like rice husks.

4.4 LABORATORY EXPERIMENTS

4.4.1 Optimum mix ratio for RH and BSG

An initial stock solution, C_0 containing both Fe^{2+} and Cu^{2+} at 3.0mg/L each at pH of 7.00 was used in this experiment. The influent was passed through a column containing a total mass of 30g of the material at flow rate of 0.06 L/min. The total mass of the adsorbent was divided using the following ratios;

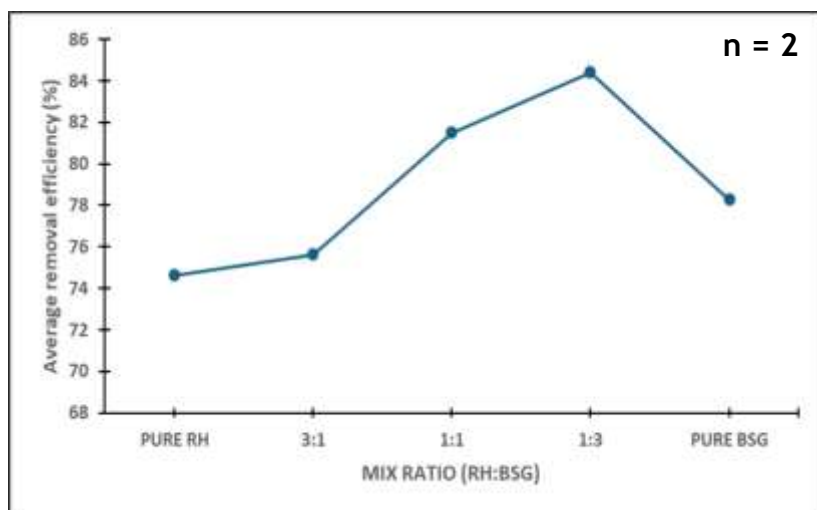


Figure 10: Average Removal efficiency against varying mix ratios

Refer to Table 7 in appendix A for the sample IDs of the raw data. The graph shows that the blend significantly influences the removal efficiencies for both copper and iron. Notably, pure RH (Sample D1) performed best for copper removal, while pure BSG (Sample D5) excelled for iron removal. However, when considering the overall performance, the 1:3, RH:BSG ratio (Sample D4) provided the best average removal efficiency. This suggests that while each adsorbent has its strong points for specific metals, the combination enhances overall performance by balancing the different adsorption characteristics. This has been interpreted as an indication that the synergistic effects in the mixed media optimize the adsorption process for a dual-contaminant solution.

4.4.2 Removal Efficiency, R_{eff} and Adsorbent Phase Concentration, Q_e

Batch experiments were carried out to determine the Adsorption kinetics of the materials. Different masses of the materials were placed in jars of water containing a 500ml solution with the heavy metals at a concentration of 3.0 mg/L each and were stirred for 90 minutes at 150 RPM.

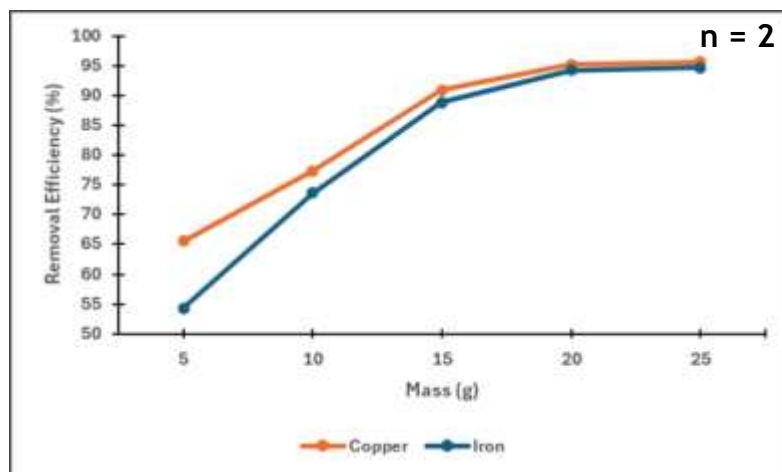


Figure 11: Removal Efficiency against varying masses

Refer to Table 8 in appendix A for the sample IDs of the raw data. The graphs demonstrated a clear trend that increasing the mass of the adsorbent from **5g** to **20g** results in a significant improvement in the removal efficiency for both copper and iron. Beyond **20g**, however, the graphs level off indicating that adding more adsorbent does not yield further meaningful gains. This plateau effect underscores the presence of an optimum adsorbent dosage, after which the system becomes less efficient, likely due to saturation of available active sites.

4.4.3 Adsorption isotherms

$$Q_e = \frac{V}{M} (C_o - C_e)$$

4.4.3.1 Langmuir Adsorption isotherms

For Copper

Table 2: Results for the Langmuir Isotherm for copper

Sample ID	Units	1	2	3	4	5
Final concentration, C_e	mg/L	1.231	0.682	0.274	0.144	0.131
$1/C_e$	L/mg	0.812	1.466	3.650	6.944	7.634
Adsorbent Phase Concentration, Q_e	mg/g	8.850	1.555	1.007	0.580	0.440
$1/Q_e$	g/mg	0.113	0.643	0.993	1.723	2.273

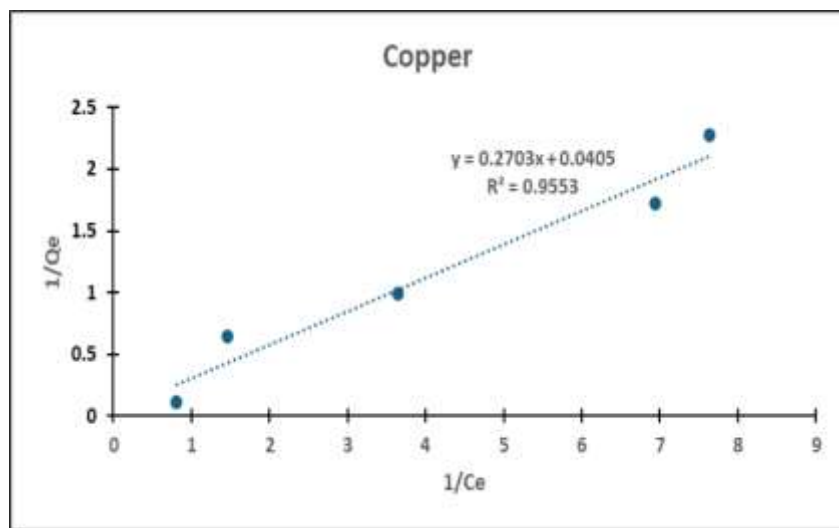


Figure 12: Copper Langmuir Isotherm Graph

$R_L = 0.150$, hence favourable (normal) Adsorption

$Q_{max} = 24.69 \text{ mg/g}$, Maximum adsorption capacity for Copper from the graph

For Iron

Table 3: Results for the Langmuir Isotherm for iron

Sample ID	Units	1	2	3	4	5
Final concentration, C_e	mg/L	1.372	0.791	0.331	0.174	0.163
$1/C_e$	L/mg	0.729	1.264	3.021	5.747	6.135
Adsorbent Phase Concentration, Q_e	mg/g	4.717	3.165	1.912	1.073	0.756
$1/Q_e$	g/mg	0.212	0.316	0.523	0.932	1.323

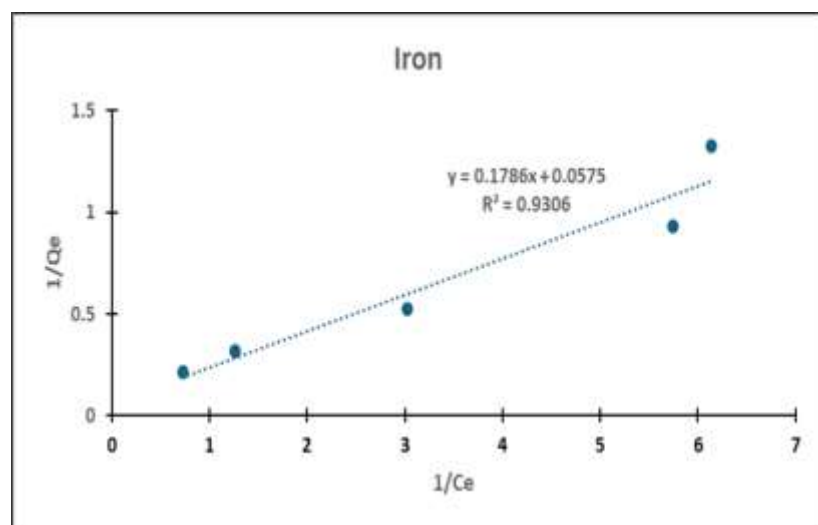


Figure 13: Iron Langmuir Isotherm Graph

$R_L = 0.322$, hence favourable (normal) Adsorption

$Q_{max} = 17.39 \text{ mg/g}$, Maximum adsorption capacity for Iron from the graph

4.4.3.2 Freundlich Adsorption isotherms

For Copper

Table 4: Results for the Freundlich Isotherm for copper

Sample ID	Units	1	2	3	4	5
Final concentration, C_e	mg/L	1.231	0.682	0.274	0.144	0.131
$\ln C_e$		0.208	-0.383	-1.295	-1.938	-2.033
Adsorbent Phase Concentration, Q_e	mg/g	8.850	1.555	1.007	0.580	0.440
$\ln Q_e$		2.180	0.441	0.007	-0.545	-0.821

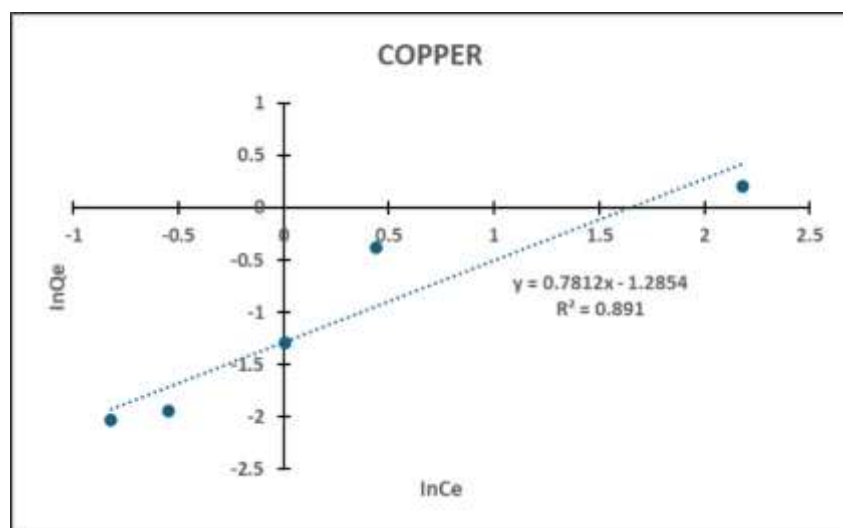


Figure 14: Copper Freundlich Isotherm Graph

$n = 0.877$ hence adsorption with chemical interaction

$\frac{1}{n} = 1.1414$ hence unfavourable / cooperative Adsorption process

For Iron

Table 5: Results for the Freundlich Isotherm for iron

Sample ID	Units	1	2	3	4	5
Final concentration, C_e	mg/L	1.372	0.791	0.331	0.174	0.163
$\ln C_e$		0.316	-0.234	-1.106	-1.749	-1.814
Adsorbent Phase Concentration, Q_e	mg/g	4.717	3.165	1.912	1.073	0.756
$\ln Q_e$		1.551	1.152	0.648	0.070	-0.280

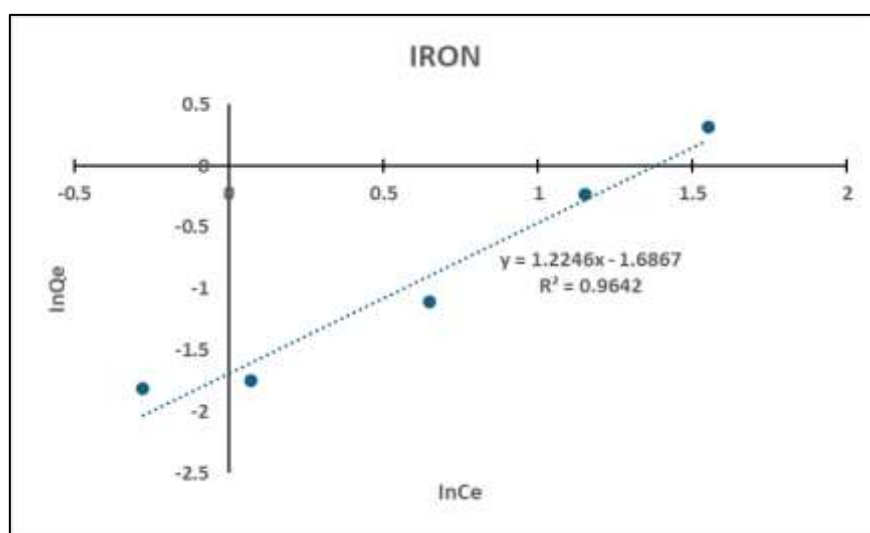


Figure 15: Iron Freundlich Isotherm Graph

$n = 1.271$ hence adsorption with physical interaction

$\frac{1}{n} = 0.787$ hence favourable adsorption process

Refer to Table 8 in appendix A for the sample IDs of the raw data. The analysis of the adsorption isotherms further elucidates the adsorption characteristics of the materials. In the Langmuir isotherm graphs for copper and iron, the linear plots indicate that both metals exhibit a favourable adsorption process, as seen by the normal adsorption trend. The maximum adsorption capacity is estimated from the slopes of these graphs, confirming that the system behaves in a predictable monolayer fashion.

In contrast, the Freundlich isotherm analysis reveals a different nuance. For copper, the negative intercept suggests that the adsorption involves a chemical interaction leading to an unfavourable or cooperative process, whereas for iron, the data imply a physical interaction with a more favourable adsorption process. These differences highlight how the underlying mechanisms can vary between contaminants, affecting how the adsorbent performs under different conditions.

4.4.4 Determining optimum mass and corresponding column height

A column experiment was carried out with varying masses of the adsorbents to determine the optimum mass for an initial concentration of solution of both copper and iron 3.0 mg/L each at a flow rate of 0.06 L/min.

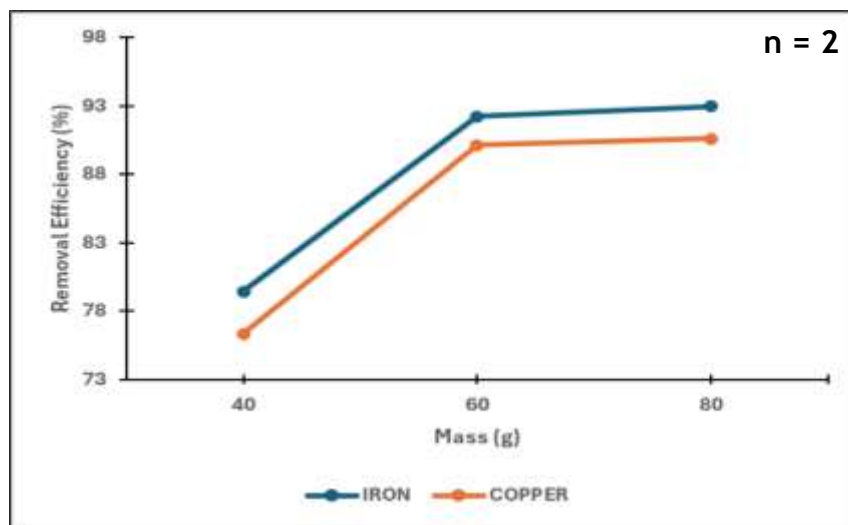


Figure 16: Optimum removal efficiency for varying masses

Refer to Table 9 in appendix A for the sample IDs of the raw data. When determining the optimum mass and corresponding column height, the related graph showed that a column packed with **60g** of adsorbent yielded high removal efficiencies for both metals approaching nearly **90% on average**. This result is particularly significant as it balances the need for high efficiency with the practical considerations of column design and material usage.

4.4.5 Breakthrough curves

A column experiment was carried out using the optimum mass attained in the previous experiment to determine the breakthrough characteristics of the mix. A sample comprised of 3.0 mg/L of copper and iron each at a pH of 7.00. The water was allowed to pass through the material at a flow rate of 0.067 L/min.

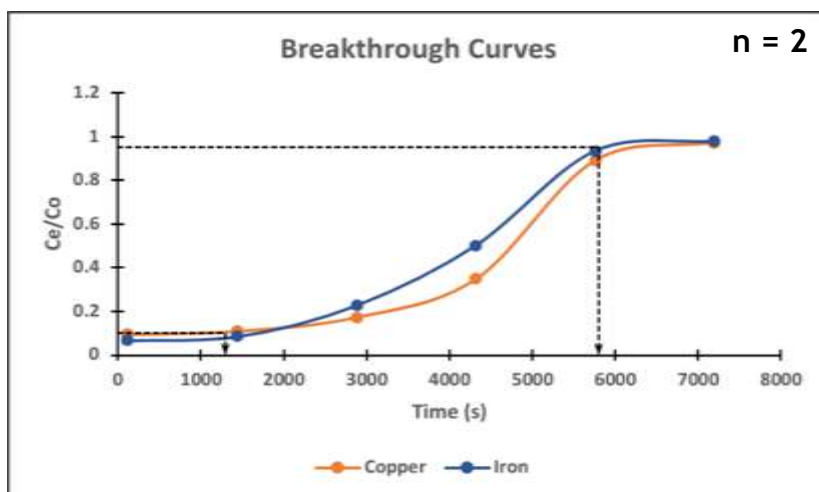


Figure 17: Breakthrough curves graph for copper and iron

Refer to Table 10 in appendix A for the sample IDs of the raw data. The breakthrough curve graphs provided insight into the dynamic performance of the adsorption system over time. The curves clearly illustrate the progression from high removal efficiencies at shorter contact times to a rapid decline as the system approaches breakthrough and eventual exhaustion. With a breakthrough time of approximately **1300 seconds** and an exhaustion time around **5800 seconds**, the graphs indicate the operational window within which the adsorbent maintains its effectiveness. This information is crucial for designing continuous treatment systems and ensuring that the adsorbent is replaced or regenerated before efficiency drops below acceptable levels.

4.5 DESIGN OF THE ADSORPTION TANK

Table 6: Summary of Random packed column dimensions

Column structure	Random packed column
Activated carbon effective size	0.6mm
Mass of adsorbent	60g
Diameter of container	6cm
Length of bed	9cm
Length of column	15cm
Volume occupied by adsorbent	254.5cm ³
Density of adsorbent	236kg/m ³
Hydraulic loading rate	12.85m/h
Empty Bed Contact Time (EBCT)/ Retention Time	85.97s
Specific Throughput	0.2859 m ³ /kg
Adsorbent usage rate	3.4977 kg/m ³

4.5.1 Small scale design

EBCT is the time the water spends in contact with the adsorbent

$$EBCT = \frac{\text{Volume occupied by adsorbent in container(cubic meters)}}{\text{Flow rate(cubic meters per second)}}$$

$$\text{Volume occupied by adsorbent} = \pi r^2 h$$

$$= \pi * (0.03)^2 * 0.09$$

$$= 2.545 * 10^{-4} m^3$$

$$EBCT = \frac{2.545 * 10^{-4} m^3}{2.96 * 10^{-6} m^3/s} = 85.97 s$$

Specific throughput is volume of water treated per unit mass of adsorbent (cubic meters per kilogram of adsorbent).

$$Specific\ throughput = \frac{Exhaustion\ time}{EBCT * Density\ of\ adsorbent}$$

$$Density\ of\ adsorbent = \frac{Mass}{Volume}$$

$$= \frac{60g}{2.545 * 10^{-4} m^3}$$

$$= 236 kg/m^3$$

$$Specific\ throughput = \frac{5800s}{85.97s * 236 kg/m^3}$$

$$= 0.2859 m^3/kg$$

Adsorbent Usage Rate is the mass of adsorbent used per volume of water.

$$Adsorbent\ Usage\ Rate = \frac{1}{Specific\ throughput}$$

$$= \frac{1}{0.2859 m^3/kg}$$

$$= 3.4977 kg/m^3$$

Hydraulic loading rate is the rate at which liquid is applied to the adsorbent volume or area.

$$Hydraulic\ loading\ rate = \frac{(Loading\ flow\ rate(m^3/hr))}{Surface\ area(m^2)}$$

$$= \frac{(0.036)m^3/hr}{0.0028m^2}$$

$$= 12.8 \text{ m/hr}$$

4.5.2 Large Scale Design

The design capacity of the system is based off the demand of a single household in Nyakasanga sub-county. According to the World Health Organization (2020), the consumption of water for households which spend more than 30 minutes in order to access water is 5.3l/c/d. For these households, it is assumed that there is total distance of more than 1000m moved to attain the water that is to and from the water source. This is termed as inadequate level of access to water. This class is also further characterized by the execution of domestic and hygienic activities such as washing/laundry, bathing etc. to be done at the source of water. Nyakasanga sub county is one such region with inadequate access to water with residents moving more than 1000m total distance to the River Nyamwamba to fetch water for use but also utilizing the river banks for washing, bathing and laundry.

Household capacity in Kasese district is at 5 people per household (UBOS, 2024). Therefore, the total demand for a singular household in this region is attained to be:

Total Demand: (5.3l/c/d * 5 people) = 26.5 litres/ day

From the adsorbent usage rate (0.1035kg/m³ calculated from the laboratory scale setup experiment, the mass of the adsorbent to be used for the household demand can be attained.

$$\text{Volume of water treated} = \frac{\text{Mass of adsorbent}}{\text{Adsorbent usage rate}}$$

$$26.5 \text{ liters} = \frac{\text{Mass of adsorbent}}{3.4977 \text{ kg/m}^3}$$

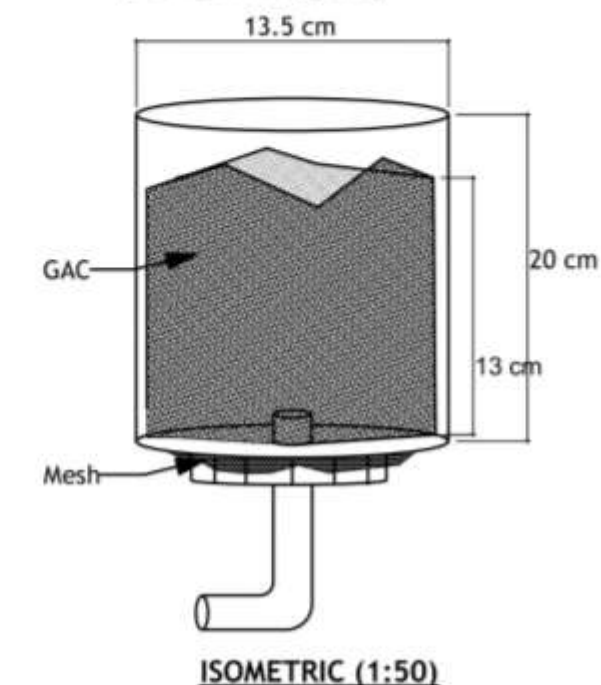
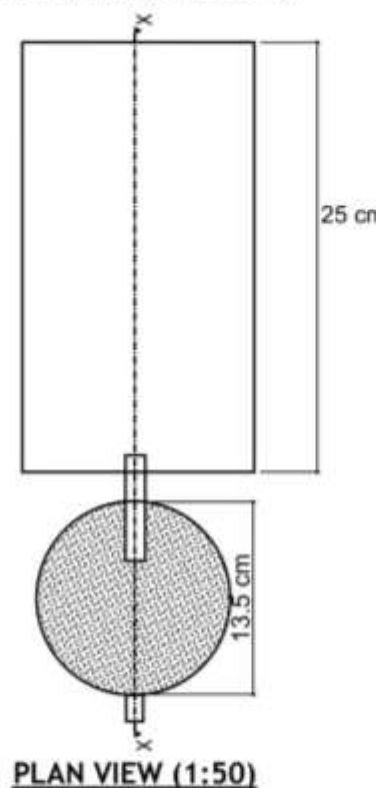
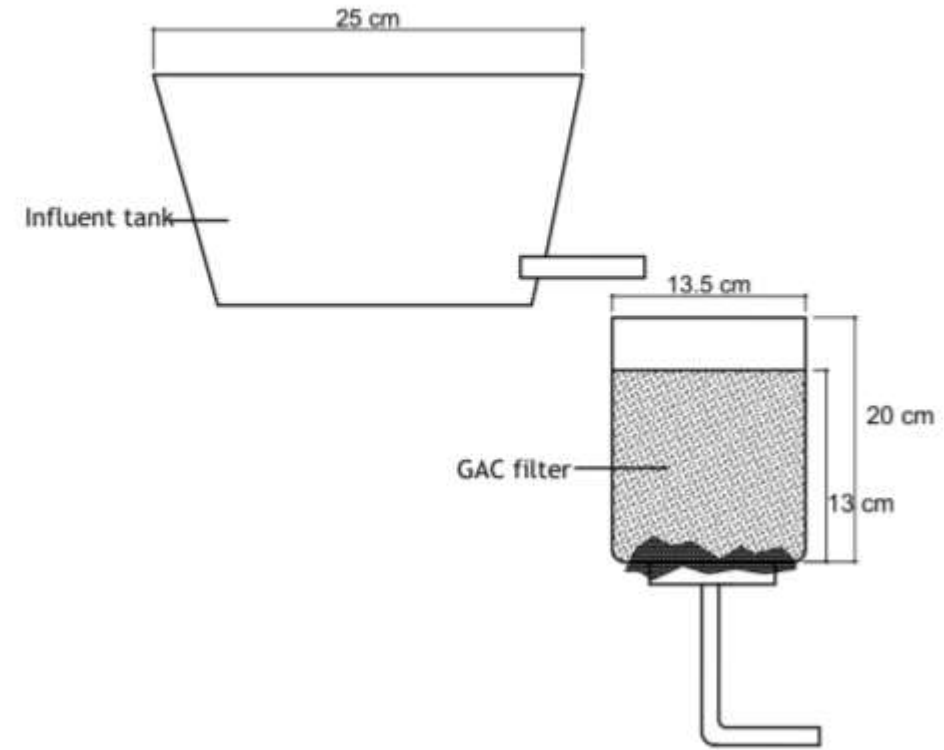
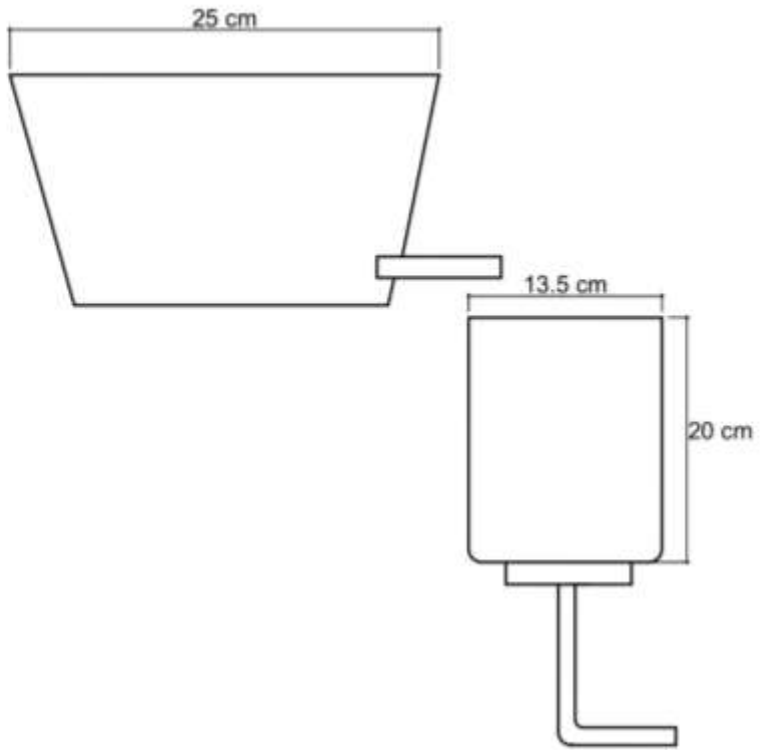
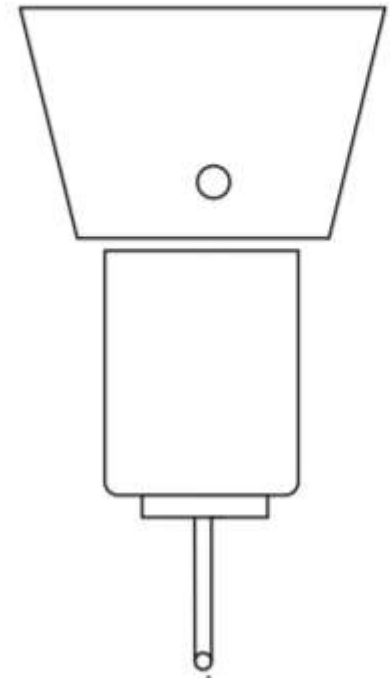
$$\text{Mass of adsorbent} = (0.0265\text{m}^3 * 3.4977\text{kg/m}^3)$$

$$= \mathbf{0.0926\text{kg}} \approx \mathbf{92.6\text{g}}$$

Therefore,

Daily consumption of 26.5 litres requires 92.6g of adsorbent

Monthly consumption of 795 litres requires 2.778kg of adsorbent



PROJECT: ASSESSING THE USE OF RH & BSG IN WATER TREATMENT

DRAWING TITLE: GAC FILTER SYSTEM

AUTHOR: KAYONGO RICHARD JEREMIAH & SSEBAGALA SANDRA

REG NUMBER : S21B32/129 & S19B32/663

CHAPTER FIVE: CONCLUSIONS AND RECOMMENDATIONS

5.1 CONCLUSIONS

From the first objective, the findings revealed a dual narrative in the water quality of River Nyamwamba. On one hand, the heavy metal concentrations, particularly copper and iron are alarmingly high exceeding the standards for potable water and posing significant health and environmental risks. On the other hand, essential physico-chemical parameters such as pH, total dissolved solids, and electrical conductivity remain within acceptable limits. This combination suggests that while the basic water matrix is largely intact, the specific issue of heavy metal contamination is acute, most notably in regions near mine tailings and active mining sites, and becomes more pronounced during wetter seasons.

From the second objective, the study demonstrated that steam activation significantly improves the performance of both rice husks and brewer's spent grain as adsorbents. By boosting the presence of functional groups like hydroxyl and silanol, this process creates additional active sites, thereby enhancing the materials' capacity to bind heavy metals. This improved chemical interaction is critical in transforming a simple physical barrier into an effective treatment medium capable of reducing hazardous metal concentrations in the water.

Based on the third objective, which combines knowledge of material composition and adsorption behaviour, the study ascertained that the 1:3 ratio (rice husks to brewer's spent grain) is the most effective combination in removing copper and iron. This ideal mix not only delivers an improved balance of surface area and active binding sites but also adheres to the principles of the Langmuir isotherm model, which suggest that the process of adsorption proceeds via a chemical mechanism

characterized by monolayer coverage. Interestingly, the findings show that copper has a higher adsorption capacity than iron, which validates the viability of further development of the treatment system for selective removal of heavy metals.

Finally, the fourth objective, the design of the adsorption system is both practical and suited to the daily water needs of a typical household. The design was guided by household water demand metrics by WHO and UBOS data ensuring relevance to actual consumption patterns, and critical design parameters such as hydraulic loading rate, retention time and adsorbent usage rate were calculated and integrated to ensure the systems' effectiveness and efficiency.

5.2 RECOMMENDATIONS

One of the key suggestions of the research is the lengthening of the sampling duration to encompass more temporal variability. By sampling over longer duration, researchers will be in a position to comprehend the different concentrations of heavy metals because of seasonal variability, especially during anomalous weather patterns like flooding. The longer duration of time would yield a more complete set of data that incorporates both short-term and long-term trends, thus enhancing the reliability of the design of the treatment system and its ability to be effective under diverse environmental conditions.

Another recommendation is the exploration of alternative means of activation of adsorbent materials, e.g., CO₂ fixation. The use of a different activation mode may enhance the surface characteristics through the introduction or supplementation of different functional groups. This avenue of research may lead to a greener and cheaper approach, perhaps with greater efficacy in heavy metal removal. A better

activation method could also reduce energy consumption or lower costs, making the treatment system more viable for broader implementation.

The study also recommends examining a wider range of mix ratios between rice husks and brewer's spent grain. Although the 1:3 ratio proved effective, testing other ratios might reveal an even more efficient combination, or at least validate the robustness of the current findings across different conditions. By broadening the scope of this investigation, future research can optimize the adsorbent mix to accommodate variations in raw water composition, ensuring that the treatment system is flexible and highly adaptable to real-world scenarios.

Finally, when it comes to designing the actual adsorption treatment system, it is recommended to explore a variety of setup configurations, such as series arrangements. This means looking at how different structural designs can influence the overall effectiveness of the system in removing heavy metals from contaminated water. By evaluating multiple configurations, engineers can identify the most efficient design that offers optimal contact between the water and the adsorbents, maximizes hydraulic retention time, and ultimately improves the system's performance. This approach could lead to a scalable and more robust solution that better meets the needs of affected communities.

REFERENCES

- Al-Ghouti, M.A. and Da'ana, D.A. (2020). Guidelines for the use and interpretation of adsorption isotherm models: A review. *Journal of Hazardous Materials*, 393, p.122383. doi:<https://doi.org/10.1016/j.jhazmat.2020.122383>.
- Alaqarbeh, M. (2021). Adsorption phenomena: Definition, mechanisms, and adsorption types: Short review. *RHAZES: Green and Applied Chemistry*, 13(0), pp.43-51. doi:<https://doi.org/10.48419/IMIST.PRSM/rhazes-v13.28283>.
- Alloway, B.J. (2013). Heavy Metals in Soils : Trace Metals and Metalloids in Soils and their Bioavailability. Dordrecht: Springer Netherlands.
- Alsawy, T., Rashad, E., El-Qelish, M. and Mohammed, R.H. (2022). A comprehensive review on the chemical regeneration of biochar adsorbent for sustainable wastewater treatment. *npj Clean Water*, 5(1). doi:<https://doi.org/10.1038/s41545-022-00172-3>.
- Amjad, M., Hussain, S., Javed, K., Rehman Khan, A. and Shahjahan, M. (2020). The Sources, Toxicity, Determination of Heavy Metals and Their Removal Techniques from Drinking Water. *World Journal of Applied Chemistry*, 5(2), p.34. doi:<https://doi.org/10.11648/j.wjac.20200502.14>.
- Apiratikul, R. and Chu, K.H. (2021). Improved fixed bed models for correlating asymmetric adsorption breakthrough curves. *Journal of Water Process Engineering*, 40, p.101810. doi:<https://doi.org/10.1016/j.jwpe.2020.101810>.

Atkinson, C.A., Jolley, D.F. and Simpson, S.L. (2007). Effect of overlying water pH, dissolved oxygen, salinity and sediment disturbances on metal release and sequestration from metal contaminated marine sediments. *Chemosphere*, 69(9), pp.1428-1437.
doi:<https://doi.org/10.1016/j.chemosphere.2007.04.068>.

Bardestani, R. and Kaliaguine, S. (2018). Steam activation and mild air oxidation of vacuum pyrolysis biochar. *Biomass and Bioenergy*, 108, pp.101-112.
doi:<https://doi.org/10.1016/j.biombioe.2017.10.011>.

Bullen, J.C., Saleesongsom, S., Gallagher, K. and Weiss, D.J. (2021). A Revised Pseudo-Second-Order Kinetic Model for Adsorption, Sensitive to Changes in Adsorbate and Adsorbent Concentrations. *Langmuir*, 37(10), pp.3189-3201.
doi:<https://doi.org/10.1021/acs.langmuir.1c00142>.

Chen, S., Qin, C., Wang, T., Chen, F., Li, X., Hou, H. and Zhou, M. (2019). Study on the adsorption of dyestuffs with different properties by sludge-rice husk biochar: Adsorption capacity, isotherm, kinetic, thermodynamics and mechanism. *Journal of Molecular Liquids*, 285, pp.62-74.
doi:<https://doi.org/10.1016/j.molliq.2019.04.035>.

Colomba, A., Franco Berruti and Briens, C. (2022). Model for the physical activation of biochar to activated carbon. *Journal of analytical and applied pyrolysis*, 168, pp.105769-105769. doi:<https://doi.org/10.1016/j.jaat.2022.105769>.

Danish, M., Ansari, K.B., Danish, M., Khatoon, A., Ali Khan Rao, R., Zaidi, S. and Ahmad Aftab, R. (2022). A comprehensive investigation of external mass transfer and intraparticle diffusion for batch and continuous adsorption of

heavy metals using pore volume and surface diffusion model. *Separation and Purification Technology*, 292, p.120996.
doi:<https://doi.org/10.1016/j.seppur.2022.120996>.

Gayathiri, M., Pulingam, T., Lee, K.T. and Sudesh, K. (2022). Activated carbon from biomass waste precursors: Factors affecting production and adsorption mechanism. *Chemosphere*, 294, p.133764.
doi:<https://doi.org/10.1016/j.chemosphere.2022.133764>.

Godson Ebenezer Adjovu, Stephen, H., James, D.E. and Ahmad, S. (2023). Measurement of Total Dissolved Solids and Total Suspended Solids in Water Systems: A Review of the Issues, Conventional, and Remote Sensing Techniques. *Remote Sensing*, 15(14), pp.3534-3534.
doi:<https://doi.org/10.3390/rs15143534>.

Goel, G. and Kaur, S. (2012). A Study on Chemical Contamination of Water Due to Household Laundry Detergents. *Journal of Human Ecology*, 38(1), pp.65-69.
doi:<https://doi.org/10.1080/09709274.2012.11906475>.

Hardie, A.G., Madubela, N., Clarke, C.E. and Lategan, E.L. (2021). Impact of powdered and liquid laundry detergent greywater on soil degradation. *Journal of Hydrology*, 595, p.126059.
doi:<https://doi.org/10.1016/j.jhydrol.2021.126059>.

Hazardous and Industrial Waste Proceedings, 29th Mid Atlantic Conference. (n.d.).
1st Edition ed. Boca Raton: CNC Press. Available at:
<https://www.taylorfrancis.com/chapters/edit/10.1201/9781003075905-23/investigation-microbial-temperature-sensitivity-effect-microorganisms->

integrity-commercial-metalworker-fluid-keith-rinkus-wei-lin-alka-jha-brian-reed.

Hu, Y., Guo, T., Ye, X., Li, Q., Guo, M., Liu, H. and Wu, Z. (2013). Dye adsorption by resins: Effect of ionic strength on hydrophobic and electrostatic interactions. *Chemical Engineering Journal*, 228, pp.392-397. doi:<https://doi.org/10.1016/j.cej.2013.04.116>.

Illingworth, J.M., Rand, B. and Williams, P.T. (2022). Understanding the mechanism of two-step, pyrolysis-alkali chemical activation of fibrous biomass for the production of activated carbon fibre matting. *Fuel Processing Technology*, 235, p.107348. doi:<https://doi.org/10.1016/j.fuproc.2022.107348>.

Irannajad, M. and Kamran Haghghi, H. (2020). Removal of Heavy Metals from Polluted Solutions by Zeolitic Adsorbents: a Review. *Environmental Processes*. doi:<https://doi.org/10.1007/s40710-020-00476-x>.

Jain, A., Kumari, S., Agarwal, S. and Khan, S. (2021). Water purification via novel nano-adsorbents and their regeneration strategies. *Process Safety and Environmental Protection*, 152, pp.441-454. doi:<https://doi.org/10.1016/j.psep.2021.06.031>.

Jareteg, A., Maggiolo, D., Thunman, H., Sasic, S. and Ström, H. (2021). Investigation of steam regeneration strategies for industrial-scale temperature-swing adsorption of benzene on activated carbon. *Chemical Engineering and Processing - Process Intensification*, 167, p.108546. doi:<https://doi.org/10.1016/j.cep.2021.108546>.

Järup, L. (2003). Hazards of heavy metal contamination. *British Medical Bulletin*, 68(1), pp.167-182. doi:<https://doi.org/10.1093/bmb/ldg032>.

Jockus Masereka, Byamugisha, D. and Adaku, C. (2022). Physicochemical Quality and Health Risks Associated with Use of Water from Nyamwamba River, Kasese, Western Uganda. *Asian Journal of Applied Chemistry Research*, 12(2), pp.19-33. doi:<https://doi.org/10.9734/ajacr/2022/v12i2217>.

Kabirizi, J. and Kato, J. (2023). *Nutritional Value of Spent Grains*. Available at: <https://www.harvestmoney.co.ug/nutritional-value-of-spent-grains/>.

Kalam, S., Abu-Khamsin, S.A., Kamal, M.S. and Patil, S. (2021). Surfactant Adsorption Isotherms: A Review. *ACS Omega*, 6(48), pp.32342-32348. doi:<https://doi.org/10.1021/acsomega.1c04661>.

Kerketta, P., Baxla, S., Gora, R., Kumari, S. and Roushan, R. (2013). Analysis of physico-chemical properties and heavy metals in drinking water from different sources in and around Ranchi, Jharkhand, India. *Veterinary World*, 6(7), p.370. doi:<https://doi.org/10.5455/vetworld.2013.370-375>.

Khan, R.A. (2022). Detergents. *Environmental Micropollutants*, pp.117-130. doi:<https://doi.org/10.1016/b978-0-323-90555-8.00014-3>.

Lei, Z., Yu, G., Dai, C. and Chen, B. (2022). Adsorption Distillation. *Special Distillation Processes*, pp.241-260. doi:<https://doi.org/10.1016/b978-0-12-820507-5.00005-1>.

Li, B. and Hausladen, D. (2023). Improving conventional household greensand treatment for efficient Mn(II) removal from drinking water. *ARPHA Conference Abstracts*, 6. doi:<https://doi.org/10.3897/aca.6.e111924>.

Li, H., Shi, A., Li, M. and Zhang, X. (2013). Effect of pH, Temperature, Dissolved Oxygen, and Flow Rate of Overlying Water on Heavy Metals Release from Storm Sewer Sediments. *Journal of Chemistry*, 2013, pp.1-11. doi:<https://doi.org/10.1155/2013/434012>.

Li, W., Deng, Y., Wang, H., Hu, Y. and Cheng, H. (2024). Potential risk, leaching behavior and mechanism of heavy metals from mine tailings under acid rain. *Chemosphere*, 350, pp.140995-140995. doi:<https://doi.org/10.1016/j.chemosphere.2023.140995>.

Lima, E.C., Mohammad Hadi Dehghani, Ashish Guleria, Sher, F., Rama Rao Karri, Guilherme Luiz Dotto and Tran, H.T. (2021). Adsorption: Fundamental aspects and applications of adsorption for effluent treatment. *Elsevier eBooks*, pp.41-88. doi:<https://doi.org/10.1016/b978-0-323-85768-0.00004-x>.

Liu, B., Xi, F., Zhang, H., Peng, J., Sun, L. and Zhu, X. (2024). Coupling machine learning and theoretical models to compare key properties of biochar in adsorption kinetics rate and maximum adsorption capacity for emerging contaminants. *Bioresource Technology*, 402, pp.130776-130776. doi:<https://doi.org/10.1016/j.biortech.2024.130776>.

Mahesh, N., Balakumar, S., Shyamalagowri, S., Manjunathan, J., Pavithra, M.K.S., Babu, P.S., Kamaraj, M. and Govarthanan, M. (2022). Carbon-based adsorbents as proficient tools for the removal of heavy metals from aqueous

solution: A state of art-review emphasizing recent progress and prospects.

Environmental Research, 213, p.113723.

doi:<https://doi.org/10.1016/j.envres.2022.113723>.

Mahmood, A.S.N., Brammer, J.G., Hornung, A., Steele, A. and Poulston, S. (2013).

The intermediate pyrolysis and catalytic steam reforming of Brewers spent grain. *Journal of Analytical and Applied Pyrolysis*, 103, pp.328-342.

doi:<https://doi.org/10.1016/j.jaat.2012.09.009>.

Mehdi, R., Khoja, A.H., Naqvi, S.R., Gao, N. and Amin, N.A.S. (2022). A Review on

Production and Surface Modifications of Biochar Materials via Biomass Pyrolysis Process for Supercapacitor Applications. *Catalysts*, 12(7), p.798.

doi:<https://doi.org/10.3390/catal12070798>.

Moghadam, P.Z., Chung, Y.G. and Snurr, R.Q. (2024). Progress toward the computational discovery of new metal-organic framework adsorbents for energy applications. *Nature energy*. doi:<https://doi.org/10.1038/s41560-023-01417-2>.

Moradi, O. and Sharma, G. (2021). Emerging novel polymeric adsorbents for removing dyes from wastewater: A comprehensive review and comparison with other adsorbents. *Environmental Research*, 201, p.111534.

doi:<https://doi.org/10.1016/j.envres.2021.111534>.

Morgan, W.J., Anstine, D.M. and Colina, C.M. (2022). Temperature Effects in Flexible Adsorption Processes for Amorphous Microporous Polymers. *The Journal of Physical Chemistry B*, 126(33), pp.6354-6365.

doi:<https://doi.org/10.1021/acs.jpca.2c04543>.

Morgana Macena, Pereira, H., Luísa Cruz-Lopes, Grosche, L. and Esteves, B. (2025).

Competitive Adsorption of Metal Ions by Lignocellulosic Materials: A Review of Applications, Mechanisms and Influencing Factors. *Separations*, 12(3), pp.70-70. doi:<https://doi.org/10.3390/separations12030070>.

Mwesigye, A.R. and Lawrence, O.B. (2023). Trace Elements Contamination of Kilembe Copper Mine Catchment Soils in Kasese District, Western Uganda. *Soil and Sediment Contamination: An International Journal*, pp.1-12. doi:<https://doi.org/10.1080/15320383.2023.2195512>.

N'diaye, A.D., Kankou, M.S.A., Hammouti, B., Nandiyanto, A.B.D. and Al Husaeni, D.F. (2022). A review of biomaterial as an adsorbent: From the bibliometric literature review, the definition of dyes and adsorbent, the adsorption phenomena and isotherm models, factors affecting the adsorption process, to the use of typha species waste as adsorbent. *Communications in Science and Technology*, 7(2), pp.140-153. doi:<https://doi.org/10.21924/cst.7.2.2022.977>.

NBL (2024). *Who We Are - Nile Breweries*. Nilebreweries.com. Available at: <https://www.nilebreweries.com/who-we-are/>.

Nekita Boraah, Sumedha Chakma and Kaushal, P. (2023). Remediation of toxic contaminants from groundwater using low-cost adsorbent. *Remediation of Toxic Contaminants from Groundwater Using low-cost Adsorbent*. doi:<https://doi.org/10.5194/egusphere-egu23-559>.

None Renu and Thandiwe Sithole (2024). A review on regeneration of adsorbent and recovery of metals: Adsorbent disposal and regeneration mechanism. *South*

African Journal of Chemical Engineering, 50, pp.39-50.

doi:<https://doi.org/10.1016/j.sajce.2024.07.006>.

Oyesigye , E., Godfrey, M., Kyobutungi Scovia and Metropolitan International University Research Repository Extension (2024). Access to Clean Water and Waterborne Diseases: A Case Study of Kasese District. 3(10), pp.184-197.

Available at:

https://www.researchgate.net/publication/385205599_Access_to_Clean_Water_and_Waterborne_Diseases_A_Case_Study_of_Kasese_District.

P. Márquez, A. Benítez, Chica, A.F., M.A. Martín and Caballero, A. (2022). Evaluating the thermal regeneration process of massively generated granular activated carbons for their reuse in wastewater treatments plants. *Journal of cleaner production*, 366, pp.132685-132685.

doi:<https://doi.org/10.1016/j.jclepro.2022.132685>.

P.U. Nzereogu, Omah, A.D., Ezema, F.I., Iwuoha, E.I. and Nwanya, A.C. (2023). Silica extraction from rice husk: Comprehensive review and applications. *Hybrid Advances*, 4, pp.100111-100111.

doi:<https://doi.org/10.1016/j.hybadv.2023.100111>.

Panwar, N.L. and Pawar, A. (2020). Influence of activation conditions on the physicochemical properties of activated biochar: a review. *Biomass Conversion and Biorefinery*. doi:<https://doi.org/10.1007/s13399-020-00870-3>.

Pereira, F., Giselle, Rita, Santana and Pereira, A.F. (2024). Use of biochar produced from brewer's spent grains as an adsorbent. *Biomass Conversion and Biorefinery*. doi:<https://doi.org/10.1007/s13399-024-06366-8>.

Premchand, P., Demichelis, F., Galletti, C., Chiaramonti, D., Bensaid, S., Antunes, E. and Fino, D. (2024). Enhancing biochar production: A technical analysis of the combined influence of chemical activation (KOH and NaOH) and pyrolysis atmospheres (N₂/CO₂) on yields and properties of rice husk-derived biochar. *Journal of Environmental Management*, 370, p.123034. doi:<https://doi.org/10.1016/j.jenvman.2024.123034>.

Priya, A.K., Yogeshwaran, V., Rajendran, S., Hoang, T.K.A., Soto-Moscoso, M., Ghfar, A.A. and Bathula, C. (2022). Investigation of mechanism of heavy metals (Cr⁶⁺, Pb²⁺& Zn²⁺) adsorption from aqueous medium using rice husk ash: Kinetic and thermodynamic approach. *Chemosphere*, 286, p.131796. doi:<https://doi.org/10.1016/j.chemosphere.2021.131796>.

Rajahmundry, G.K., Garlapati, C., Kumar, P.S., Alwi, R.S. and Vo, D.-V.N. (2021). Statistical analysis of adsorption isotherm models and its appropriate selection. *Chemosphere*, 276, p.130176. doi:<https://doi.org/10.1016/j.chemosphere.2021.130176>.

Rozanov, L.N. (2021). Kinetic equations of non-localized physical adsorption in vacuum for Freundlich adsorption isotherm. *Vacuum*, 189, p.110267. doi:<https://doi.org/10.1016/j.vacuum.2021.110267>.

Saad Alafnan, Awotunde, A.A., Glatz, G., Stephen Baffour Adjei, Ibrahim Alrumaih and Gowida, A. (2021). Langmuir adsorption isotherm in unconventional

resources: Applicability and limitations. 207, pp.109172-109172.
doi:<https://doi.org/10.1016/j.petrol.2021.109172>.

Sabadash, V. and Lysko, V. (2023). Studies on Adsorption of Petroleum Products in Static Conditions. *Journal of Ecological Engineering*, 24(10), pp.40-46.
doi:<https://doi.org/10.12911/22998993/169997>.

SADEGHI, S.H.R., HARCHEGANI, M.K. and YOUNESI, H.A. (2012). Suspended sediment concentration and particle size distribution, and their relationship with heavy metal content. *Journal of Earth System Science*, 121(1), pp.63-71.
doi:<https://doi.org/10.1007/s12040-012-0143-4>.

Sakhiya, A.K., Baghel, P., Anand, A., Vijay, V.K. and Kaushal, P. (2021). A comparative study of physical and chemical activation of rice straw derived biochar to enhance Zn+2 adsorption. *Bioresource Technology Reports*, 15, p.100774. doi:<https://doi.org/10.1016/j.biteb.2021.100774>.

Siddha, S. and Kumar, M. (2024). Sustainable approaches for heavy metal removal from water. *Role of Green Chemistry in Ecosystem Restoration to Achieve Environmental Sustainability*, pp.227-235.
doi:<https://doi.org/10.1016/b978-0-443-15291-7.00023-7>.

Singh, M., Ansari, A.A., Müller, G. and Singh, I.B. (1997). Heavy metals in freshly deposited sediments of the Gomati River (a tributary of the Ganga River): effects of human activities. *Environmental Geology*, 29(3-4), pp.246-252.
doi:<https://doi.org/10.1007/s002540050123>.

Somi Doja, Lava Kumar Pillari and Bichler, L. (2021). Processing and activation of tire-derived char: A review. *Renewable and Sustainable Energy Reviews*, 155, pp.111860-111860. doi:<https://doi.org/10.1016/j.rser.2021.111860>.

Sonmez Baghirzade, B., Zhang, Y., Reuther, J.F., Saleh, N.B., Venkatesan, A.K. and Apul, O.G. (2021). Thermal Regeneration of Spent Granular Activated Carbon Presents an Opportunity to Break the Forever PFAS Cycle. *Environmental Science & Technology*, 55(9), pp.5608-5619. doi:<https://doi.org/10.1021/acs.est.0c08224>.

Tchounwou, P.B., Yedjou, C.G., Patlolla, A.K. and Sutton, D.J. (2014). Heavy Metal Toxicity and the Environment. *Experientia Supplementum*, 101(1), pp.133-164. doi:https://doi.org/10.1007/978-3-7643-8340-4_6.

Topare, N.S. and Wadgaonkar, V.S. (2022). A review on application of low-cost adsorbents for heavy metals removal from wastewater. *Materials Today: Proceedings*. doi:<https://doi.org/10.1016/j.matpr.2022.08.450>.

Velempini, T., Ahamed, MEH. and Pillay, K. (2023). Heavy-metal spent adsorbents reuse in catalytic, energy and forensic applications- a new approach in reducing secondary pollution associated with adsorption. *Results in Chemistry*, 5, p.100901. doi:<https://doi.org/10.1016/j.rechem.2023.100901>.

Wanyama, J., Bwambale, E. and Nakawuka, P. (2024). Comparative performance assessment of pilot irrigation schemes in Uganda. *Heliyon*, 10(10), p.e31600. doi:<https://doi.org/10.1016/j.heliyon.2024.e31600>.

Wierzba, S. and Kłos, A. (2019). Heavy metal sorption in biosorbents - Using spent grain from the brewing industry. *Journal of Cleaner Production*, 225, pp.112-120. doi:<https://doi.org/10.1016/j.jclepro.2019.03.286>.

Wilber, M., Jane, Y., Morgan, A. and Kasangaki, A. (2020). HEAVY METAL POLLUTION IN THE MAIN RIVERS OF RWENZORI REGION, KASESE DISTRICT SOUTH-WESTERN UGANDA. *Jour. Env. Res.*, 8(3), pp.78-090. Available at: http://sciencebeingjournal.com/sites/default/files/02_0803_MW01.pdf

Wiśniewska, M., Rejer, K., Pietrzak, R. and Nowicki, P. (2022). Biochars and Activated Biocarbons Prepared via Conventional Pyrolysis and Chemical or Physical Activation of Mugwort Herb as Potential Adsorbents and Renewable Fuels. *Molecules*, 27(23), p.8597. doi:<https://doi.org/10.3390/molecules27238597>.

Yildiz, H. (2024). The production of a novel adsorbent from forest waste (*Platanus orientalis* L.) for dye adsorption: Adsorption process optimization and experimental design. *Materials Science and Engineering B*, 304, pp.117366-117366. doi:<https://doi.org/10.1016/j.mseb.2024.117366>.

Zhang, C., Yu, Z., Zeng, G., Jiang, M., Yang, Z., Cui, F., Zhu, M., Shen, L. and Hu, L. (2014). Effects of sediment geochemical properties on heavy metal bioavailability. *Environment International*, 73, pp.270-281. doi:<https://doi.org/10.1016/j.envint.2014.08.010>.

Zhang, P., Duan, W., Peng, H., Pan, B. and Xing, B. (2021). Functional Biochar and Its Balanced Design. *ACS Environmental Au*, 2(2), pp.115-127. doi:<https://doi.org/10.1021/acsenvironau.1c00032>.

Zhao, W., Cheng, Y., Yuan, M. and An, F. (2014). Effect of Adsorption Contact Time on Coking Coal Particle Desorption Characteristics. *Energy & Fuels*, 28(4), pp.2287-2296. doi:<https://doi.org/10.1021/ef402093g>.

Zhou, W., Meng, X., Gao, J., Zhao, H., Zhao, G. and Ma, J. (2021). Electrochemical regeneration of carbon-based adsorbents: a review of regeneration mechanisms, reactors, and future prospects. *Chemical Engineering Journal Advances*, 5, p.100083. doi:<https://doi.org/10.1016/j.cejadv.2020.100083>.

Zhu, H., Xu, J., Zhou, B., Ren, J., Yang, Q., Wang, Z. and Nie, W. (2022). Leaching Characteristics of Potentially Toxic Metals from Tailings at Lujiang Alum Mine, China. *International Journal of Environmental Research and Public Health*, 19(24), pp.17063-17063. doi:<https://doi.org/10.3390/ijerph192417063>.

APPENDICES

APPENDIX A: TABLES OF RESULTS

Table 7: Results from variation of different mix ratios of adsorbents in column experiment

Sample ID (RH:BSG)	Units	D1 Pure RH	D2 (3:1)	D3 (1:1)	D4 (1:3)	D5 Pure BSG
COPPER						
Final Cu ²⁺ Concentration	mg/L	0.243	0.331	0.402	0.428	0.921
Removal Efficiency for Cu ²⁺	%	91.90	88.97	86.60	85.73	69.30
IRON						
Final Fe ²⁺ Concentration	mg/L	1.280	1.131	0.709	0.508	0.383
Removal Efficiency for Fe ²⁺	%	57.33	62.30	76.37	83.07	87.23
Average Removal Efficiency	%	74.62	75.64	81.49	84.40	78.27

Table 8: Results from variation of mass of adsorbent at 150rpm for 90 minutes contact time

Sample ID	Units	E1	E2	E3	E4	E5
Volume of Solution, V	L	0.500	0.500	0.500	0.500	0.500
Adsorbent Mass, M	g	5	10	15	20	25
COPPER						
Cu ²⁺ Initial concentration, C _o	mg/L	3.00	3.00	3.00	3.00	3.00
Cu ²⁺ Final concentration, C _e	mg/L	1.231	0.682	0.274	0.144	0.131
Removal Efficiency, R _{eff}	%	65.57	77.27	90.87	95.17	95.63
IRON						
Fe ²⁺ Initial concentration, C _o	mg/L	3.00	3.00	3.00	3.00	3.00
Fe ²⁺ Final concentration, C _e	mg/L	1.372	0.791	0.331	0.174	0.163
Removal Efficiency, R _{eff}	%	54.27	73.63	88.80	94.20	94.63

Table 9: Results from the varying column masses and corresponding heights

Sample ID	Units	F1	F2	F3
Adsorbent mass, M	g	40	60	80
COPPER				
Cu^{2+} Initial concentration, C_o	mg/L	3.00	3.00	3.00
Cu^{2+} Final concentration, C_e	mg/L	0.710	0.321	0.301
Removal Efficiency, R_{eff}	%	76.33	89.30	89.97
IRON				
Fe^{2+} Initial concentration, C_o	mg/L	3.00	3.00	3.00
Fe^{2+} Final concentration, C_e	mg/L	0.617	0.234	0.212
Removal Efficiency, R_{eff}	%	79.43	92.20	92.93
Average Removal Efficiency, R_{eff}	%	77.88	90.75	91.45

Table 10: Results from the breakthrough curves experiment

Sample ID	Units	G1	G2	G3	G4	G5	G6
Time	s	120	1440	2880	4320	5760	7200
COPPER							
Cu^{2+} Initial concentration, C_o	mg/L	3.00	3.00	3.00	3.00	3.00	3.00
Cu^{2+} Final concentration, C_e	mg/L	0.284	0.327	0.520	1.045	2.675	2.915
C_e/C_o	-	0.095	0.109	0.173	0.348	0.892	0.972
Percentage Removal	%	90.53	89.10	82.67	65.17	10.83	2.83
IRON							
Fe^{2+} Initial concentration, C_o	mg/L	3.00	3.00	3.00	3.00	3.00	3.00
Fe^{2+} Final concentration, C_e	mg/L	0.204	0.256	0.685	1.505	2.805	2.940
C_e/C_o	-	0.068	0.085	0.228	0.502	0.935	0.980
Percentage Removal	%	93.20	91.47	77.17	49.83	6.50	2.00

APPENDIX B: PICTORIAL



Figure 18: Sediment sampling



Figure 19: Water column sampling



Figure 20: Residents washing from river



Figure 21: In situ testing with multimeter



Figure 22: Sealed material in pots



Figure 23: Activated BSG and RH



Figure 24: Sieving materials



Figure 25: Material mass ratios



Figure 26: Batch experiment set up



Figure 27: Analytical Reagents



Figure 28: Setting up column bed



Figure 29: Filtering samples



Figure 30: Laboratory setup



Figure 31: Prototype setup

APPENDIX C: CERTIFICATES OF ANALYSIS

Telephone
+256 (0) 414 250 464 (Gen)
+256 (0) 414 250 474
Email: dgal@mia.go.ug
Website: www.mia.go.ug

In any Correspondence on
this subject please
quote No.....



DFD 292/2024

MINISTRY OF INTERNAL AFFAIRS
DIRECTORATE OF GOVERNMENT
ANALYTICAL LABORATORY
Plot No. 2 Lourdel Road
Wandegeya,
P.O. Box 105639
Kampala - Uganda

04th December 2024

MR. KAYONGO RICHARD JEREMIAH AND MS SSEBAGALA SANDRA
REG NO. S21B32/129 & S19B32/663
UGANDA CHRISTIAN UNIVERSITY
P.O BOX 4,
MUKONO-UGANDA
Tel: 256-778-051449

REPORT OF ANALYSIS

Description of the Samples

Three samples of water were received from Mr. Kayongo Richard Jeremiah, on 18th November 2024 and was analysed from 22nd to 28th November 2024. A summary of the sample received is shown in table below.

S/N	Description	Quantity	Assigned Lab ID
1	Three water Samples packed in plastic water bottles from Nyamwamba River (Kasese District)	03	Samples "A1, B1, &C1" DFD 292/2024

Analysis Requested

To determine the Iron and Copper contents.

Method of Analysis

Analysis of Iron and Copper were analysed using AAS method.

Results of Analysis

The results are summarized in the table below:

Test/Parameter	Units	Results for DFD 292/2024			US EAS 12:2014
		Sample "A1"	Sample "B1"	Sample "C1"	
Iron (Fe)	mg/L	2.865	2.827	2.114	0.3 Max
Copper (Cu)	mg/L	2.904	2.036	2.106	1.0 Max

Remarks

1. The samples "A1, B1, &C1" DFD 292/2024 were analysed and the results indicated in bold did **not** comply with the limit of metals specified in the Ugandan standard for US EAS 12:2014, Potable water — Specification
2. Results relate to sample analyzed and are reported as on received basis.

Fred · 04/12/24
Semalago Fredrick
Government Analyst

Telephone
+256 (0) 414 250 464 (Gen)
+256 (0) 414 250 474
Email: dgal@mia.go.ug
Website: www.mia.go.ug

In any Correspondence on
this subject please
quote No.....

DFD 008/2025



THE REPUBLIC OF UGANDA

MINISTRY OF INTERNAL AFFAIRS
DIRECTORATE OF GOVERNMENT
ANALYTICAL LABORATORY
Plot No. 2 Lourdel Road
Wandegeya,
P.O. Box 105639
Kampala - Uganda

16th January 2025

MR. KAYONGO RICHARD JEREMIAH AND MS SSEBAGALA SANDRA
REG NO. S21B32/129 & S19B32/663
UGANDA CHRISTIAN UNIVERSITY
P.O BOX 4,
MUKONO-UGANDA
Tel: 256-778-051449

REPORT OF ANALYSIS

Description of the Samples

Three samples of water were received from Mr. Kayongo Richard Jeremiah, on 07th January 2025 and was analysed from 08th to 13th January 2025. A summary of the sample received is shown in table below

S/N	Description	Quantity	Assigned Lab ID
1	Three water Samples packed in plastic water bottles from Nyamwamba River (Kasese District)	03	Samples "A2, B2, &C2" DFD 008/2025

Analysis Requested

To determine the Iron and Copper contents.

Method of Analysis

Analysis of Iron and Copper were analysed using AAS method.

Results of Analysis

The results are summarized in the table below:

Test/Parameter	Units	Results for DFD 008/2025			US EAS 12:2014
		Sample "A2"	Sample "B2"	Sample "C2"	
Iron (Fe)	mg/L	2.661	2.397	2.531	0.3 Max
Copper (Cu)	mg/L	1.857	1.559	1.773	1.0 Max

Remarks

1. The samples "A2, B2, &C2" DFD 008/2025 were analysed and the results indicated in bold did **not** to comply with the limit of metals specified in the Ugandan standard for US EAS 12:2014, Potable water — Specification
2. Results relate to sample analyzed and are reported as on received basis.

S. S. S. - 16/01/25
Semalago Fredrick
Government Analyst

"Go Scientific for a Safe and Just Society"

Page 1 of 1

Telephone
+256 (0) 414 250 464 (Gen)
+256 (0) 414 250 474
Email: dgal@mia.go.ug
Website: www.mia.go.ug

In any Correspondence on
this subject please
quote No.....

DFD 012/2025



MINISTRY OF INTERNAL AFFAIRS
DIRECTORATE OF GOVERNMENT
ANALYTICAL LABORATORY
Plot No. 2 Lourdel Road
Wandegeya,
P.O. Box 105639
Kampala - Uganda

24th January 2025

MR. KAYONGO RICHARD JEREMIAH AND MS SSEBAGALA SANDRA
REG NO. S21B32/129 & S19B32/663
UGANDA CHRISTIAN UNIVERSITY
P.O BOX 4,
MUKONO-UGANDA
Tel: 256-778-051449

REPORT OF ANALYSIS

Description of the Samples

Three samples of water were received from Mr. Kayongo Richard Jeremiah, on 21st January 2025 and was analysed from 22nd January to 24th January 2025. A summary of the sample received is shown in table below

S/N	Description	Quantity	Assigned Lab ID
1	Three water Samples packed in plastic water bottles from Nyamwamba River (Kasese District)	03	Samples "A3, B3, &C3" DFD 012/2025

Analysis Requested

To determine the Iron and Copper contents.

Method of Analysis

Analysis of Iron and Copper were analysed using AAS method.

Results of Analysis

The results are summarized in the table below:

Test/Parameter	Units	Results for DFD 012/2025			US EAS 12:2014
		Sample "A3"	Sample "B3"	Sample "C3"	
Iron (Fe)	mg/L	2.196	1.908	2.011	0.3 Max
Copper (Cu)	mg/L	1.372	0.891	1.028	1.0 Max

Remarks

1. The samples "A3, B3, &C3" DFD 012/2025 were analysed and the results indicated in bold did **not** to comply with the limit of metals specified in the Ugandan standard for US EAS 12:2014, Potable water — Specification
2. Results relate to sample analyzed and are reported as on received basis.

S. Fred - 24/01/26

Semalago Fredrick
Government Analyst

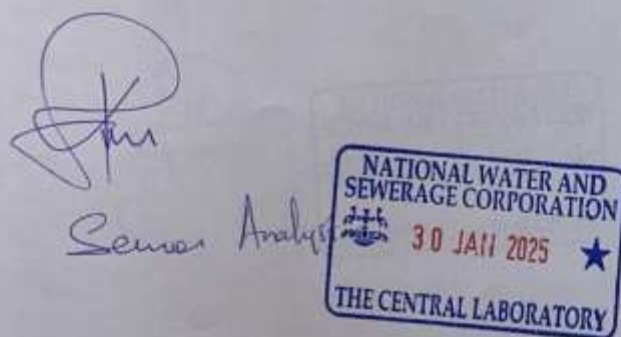
Sampled by: Kayongo Richard Jeremiah & Ssebagala Sandra

Uganda Christian University

Date of Sampling: 16th November 2024

Source: River Nyamwamba, Nyakasanga I

Parameter	A1	B1	C1
pH	6.33	6.77	6.83
EC (µS)	56.8	68.5	53.2
TDS (ppm)	39.7	47.1	37.7
Temperature (°C)	22.2	22.6	20.8
Salinity (ppt)	0.03	0.03	0.03



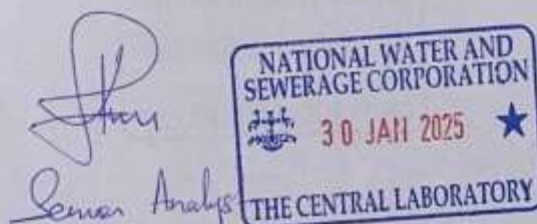
Sampled by: Kayongo Richard Jeremiah & Ssebagala Sandra

Uganda Christian University

Date of Sampling: 22nd December, 2024

Source: River Nyamwamba, Nyakasanga I

Parameter	A2	B2	C2
pH	6.6	6.83	6.34
EC (μS)	58.1	54.1	58.1
TDS (ppm)	40.0	40.1	42.8
Temperature ($^{\circ}\text{C}$)	22.8	23.0	22.9
Salinity (ppt)	0.03	0.03	0.03

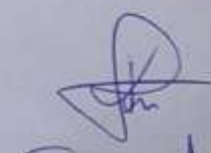


Sampled by: Kayongo Richard Jeremiah & Ssebagala Sandra
Uganda Christian University

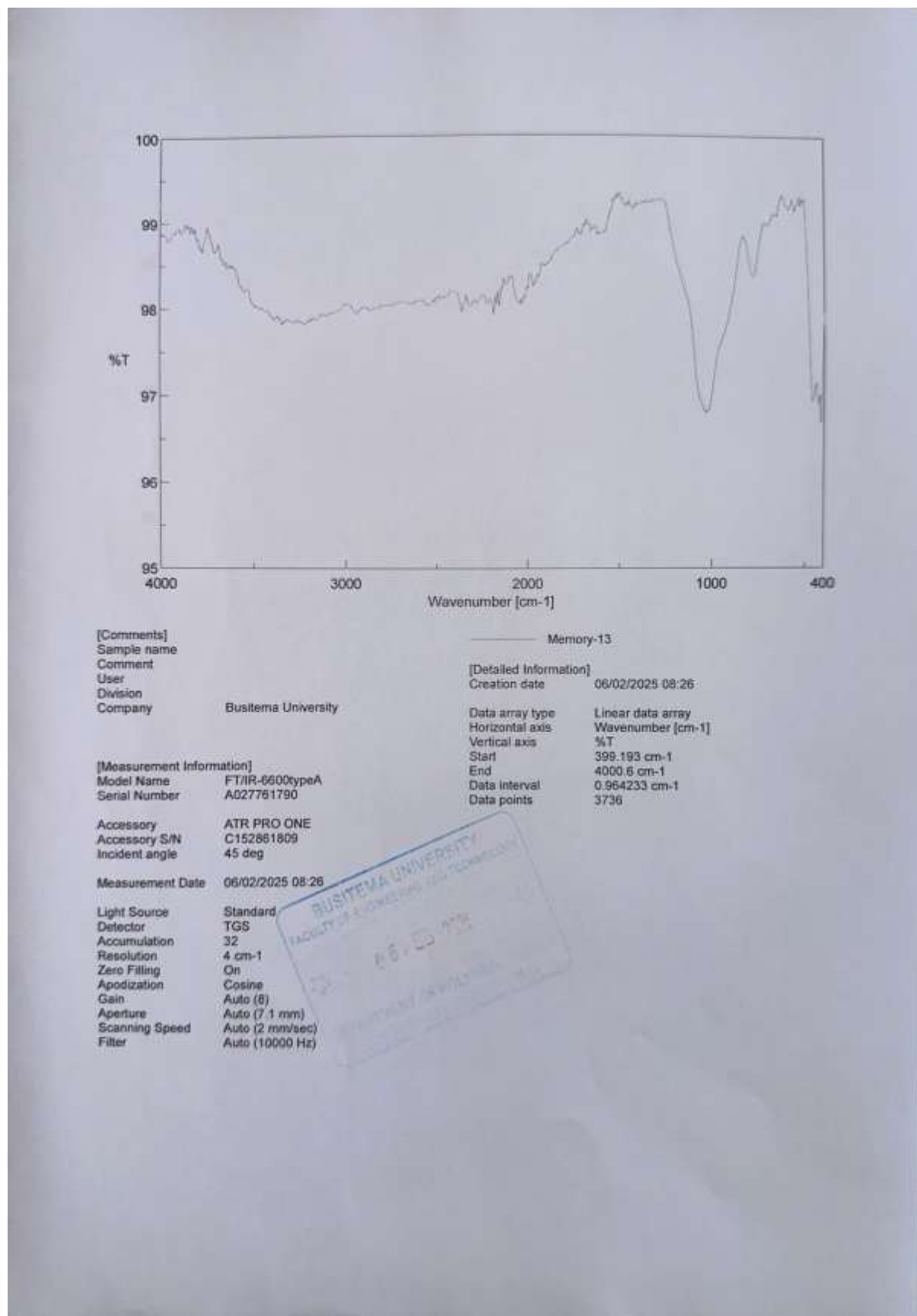
Date of Sampling: 18th January 2025

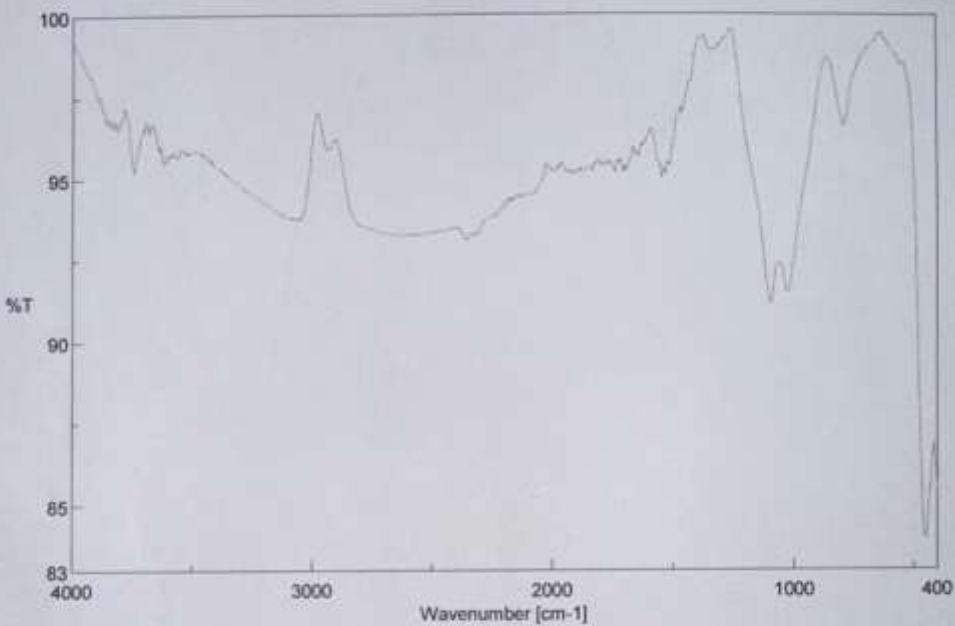
Source: River Nyamwamba, Nyakasanga I

Parameter	A3	B3	C3
pH	6.7	6.7	6.71
EC (µS)	49.7	49.3	52.3
TDS (ppm)	36.4	37.4	38.4
Temperature (°C)	23.0	23.1	22.6
Salinity (ppt)	0.03	0.03	0.03


Sandra Analyst

NATIONAL WATER AND
SEWERAGE CORPORATION
 30 JAN 2025 ★
THE CENTRAL LABORATORY





[Comments]
Sample name:
Comment:
User:
Division:
Company: Busitema University

Memory-6

[Detailed Information]
Creation date: 06/02/2025 08:18

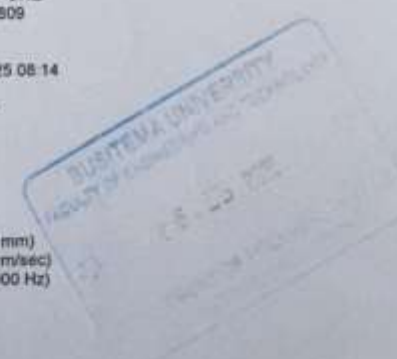
Data array type:	Linear data array
Horizontal axis:	Wavenumber [cm ⁻¹]
Vertical axis:	%T
Start:	399.193 cm ⁻¹
End:	4000.6 cm ⁻¹
Data interval:	0.964233 cm ⁻¹
Data points:	3736

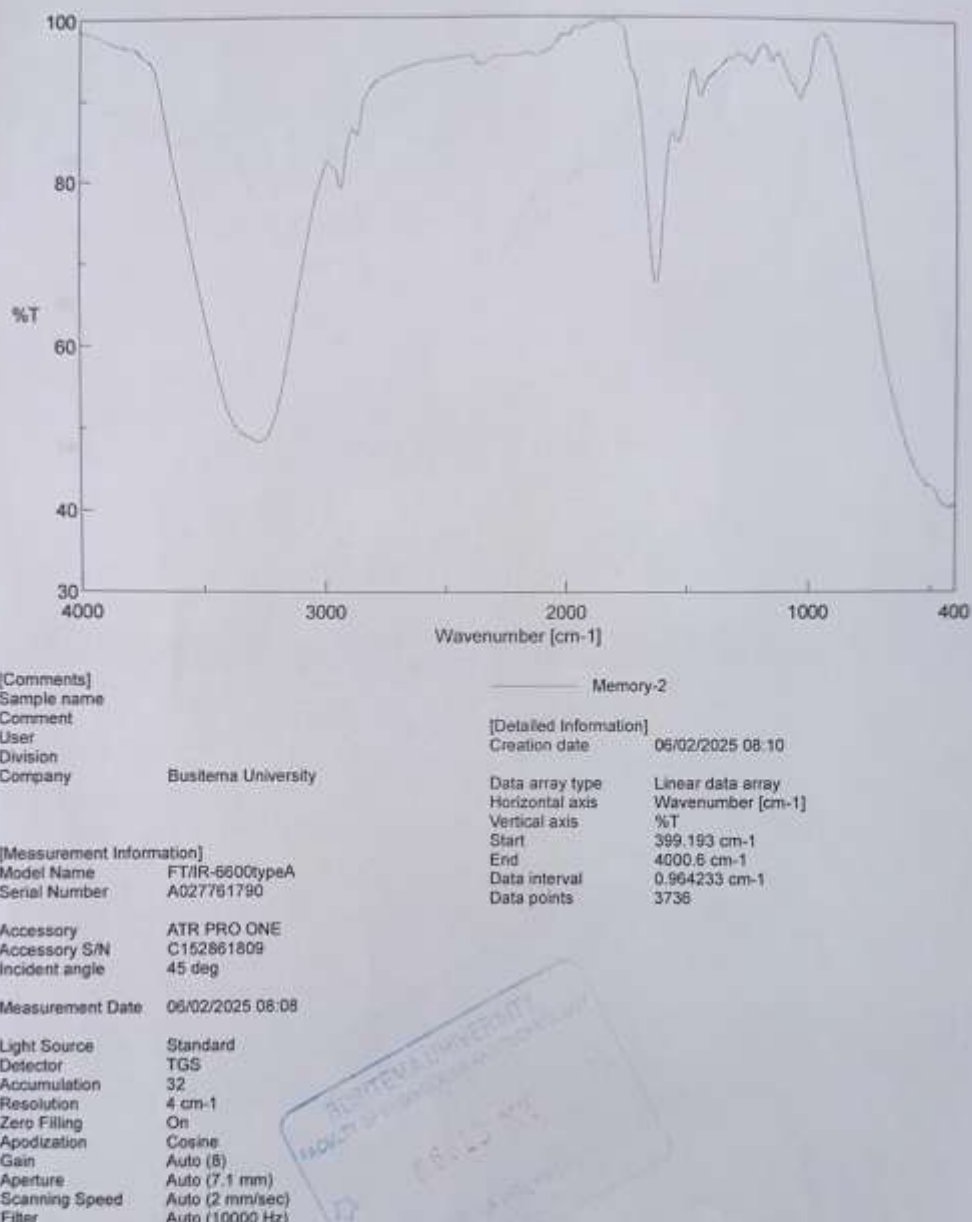
[Measurement Information]
Model Name: FT/IR-6600typeA
Serial Number: A027761790

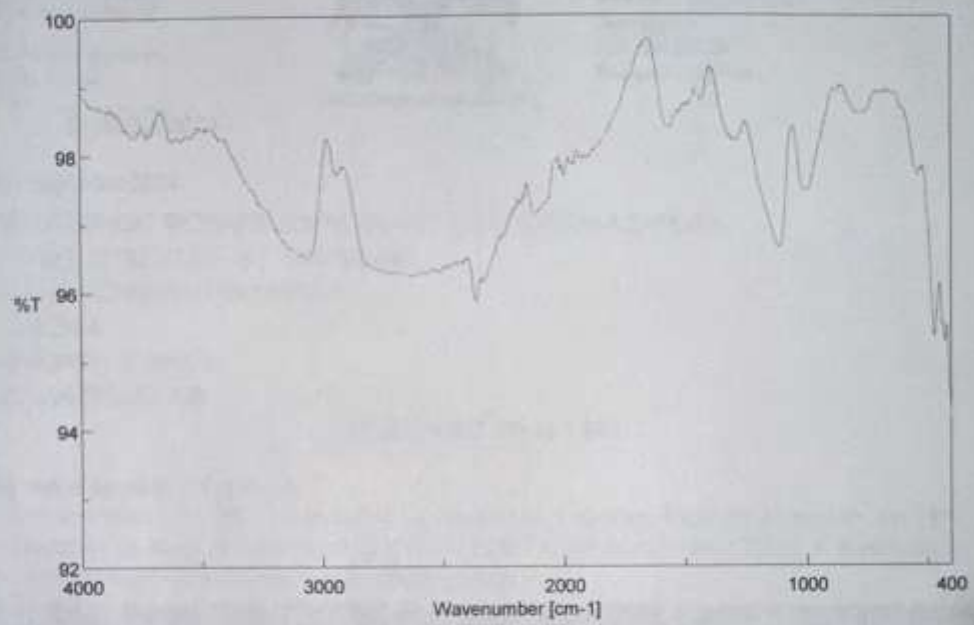
Accessory: ATR PRO ONE
Accessory S/N: C152861809
Incident angle: 45 deg

Measurement Date: 06/02/2025 08:14

Light Source: Standard
Detector: TGS
Accumulation: 32
Resolution: 4 cm⁻¹
Zero Filling: On
Apodization: Cosine
Gain: Auto (8)
Aperture: Auto (7.1 mm)
Scanning Speed: Auto (2 mm/sec)
Filter: Auto (10000 Hz)







[Comments]
 Sample name
 Comment
 User
 Division
 Company Busitema University

Memory-11

[Detailed Information]
 Creation date 06/02/2025 08:22

[Measurement Information]
 Model Name: FT/IR-6600typeA
 Serial Number: A027761790

Data array type Linear data array
 Horizontal axis Wavenumber [cm⁻¹]
 Vertical axis %T
 Start 399 193 cm⁻¹
 End 4000.6 cm⁻¹
 Data interval 0.964233 cm⁻¹
 Data points 3736

Accessory ATR PRO ONE
 Accessory S/N C152861809
 Incident angle 45 deg

Measurement Date 06/02/2025 08:21

Light Source Standard
 Detector TGS
 Accumulation 32
 Resolution 4 cm⁻¹
 Zero Filling On
 Apodization Cosine
 Gain Auto (8)
 Aperture Auto (7.1 mm)
 Scanning Speed Auto (2 mm/sec)
 Filter Auto (10000 Hz)

Telephone
+256 (0) 414 250 464 (Gen)
+256 (0) 414 250 474
Email: dgal@mia.go.ug
Website: www.mia.go.ug

In any Correspondence on
this subject please
quote No.....



DFD 060/2025

MINISTRY OF INTERNAL AFFAIRS
DIRECTORATE OF GOVERNMENT
ANALYTICAL LABORATORY
Plot No. 2 Lourdel Road
Wandegeya,
P.O. Box 105639
Kampala - Uganda

07th March 2025

MR. KAYONGO RICHARD JEREMIAH AND MS SSEBAGALA SANDRA
REG NO. S21B32/129 & S19B32/663
UGANDA CHRISTIAN UNIVERSITY
P.O BOX 4,
MUKONO-UGANDA
Tel: 256-778-051449

REPORT OF ANALYSIS

Description of the Samples

Three samples of water were received from Mr. Kayongo Richard Jeremiah, on 03rd March 2025 and was analysed from 04th to 07th March 2025. A summary of the sample received is shown in table below,

S/N	Description	Quantity	Assigned Lab ID
1	Filtrate water samples (05) packed in plastic bottles from the optimum mix ratio column test	05	Samples "D1, D2, D3, D4 & D5" DFD 060/2025

Analysis Requested

To determine the Iron and Copper contents.

Method of Analysis

Analysis of Iron and Copper were analysed using AAS method.

Results of Analysis

The results are summarized in the table below;

Test/Parameter	Units	Results for DFD 060/2025					US EAS 12:2014
		Sample "D1"	Sample "D2"	Sample "D3"	Sample "D4"	Sample "D5"	
Copper (Cu)	mg/L	0.243	0.331	0.402	0.428	0.921	1.0 Max
Iron (Fe)	mg/L	1.280	1.131	0.709	0.508	0.383	0.3 Max

Remarks

1. The samples "D1, D2, D3, D4 & D5" DFD 060/2025 were analysed and found to comply with the limit of metals (Copper) specified in the Ugandan standard for US EAS 12:2014, Potable water — Specification except (Iron) for all Samples.
2. Results relate to sample analyzed and are reported as on received basis.

Semalago Fredrick
Semalago Fredrick
Government Analyst

Telephone
+256 (0) 414 250 464 (Gen)
+256 (0) 414 250 474
Email: dgal@mia.go.ug
Website: www.mia.go.ug

In any Correspondence on
this subject please
quote No.....

DFD 061/2025



MINISTRY OF INTERNAL AFFAIRS
DIRECTORATE OF GOVERNMENT
ANALYTICAL LABORATORY
Plot No. 2 Lourdel Road
Wandegeya,
P.O. Box 105639
Kampala - Uganda

12th March 2025

MR. KAYONGO RICHARD JEREMIAH AND MS SSEBAGALA SANDRA
REG NO. S21B32/129 & S19B32/663
UGANDA CHRISTIAN UNIVERSITY
P.O BOX 4,
MUKONO-UGANDA
Tel: 256-778-051449

REPORT OF ANALYSIS

Description of the Samples

Three samples of water were received from Mr. Kayongo Richard Jeremiah, on 10th March 2025 and was analysed from 10th to 12th March 2025. A summary of the sample received is shown in table below.

S/N	Description	Quantity	Assigned Lab ID
1	Filtrate water samples (05) packed in plastic bottles from the batch test	05	Samples "E1, E2, E3, E4 & E5" DFD 061/2025

Analysis Requested

To determine the Iron and Copper contents.

Method of Analysis

Analysis of Iron and Copper were analysed using AAS method.

Results of Analysis

The results are summarized in the table below:

Test/Parameter	Units	Results for DFD 061/2025					US EAS 12:2014
		Sample "E1"	Sample "E2"	Sample "E3"	Sample "E4"	Sample "E5"	
Copper (Cu)	mg/L	1.231	0.682	0.274	0.144	0.131	1.0 Max
Iron (Fe)	mg/L	1.372	0.791	0.331	0.174	0.163	0.3 Max

Remarks

1. The samples "E1, E2, E3, E4 & E5" DFD 061/2025 were analysed and found to comply with the limit of metals specified in the Ugandan standard for US EAS 12:2014, Potable water — Specification except Samples E1 & E2"
2. Results relate to sample analyzed and are reported as on received basis.

Fred . 12/03/25

Semalago Fredrick
Government Analyst

Telephone
+256 (0) 414 250 464 (Gen)
+256 (0) 414 250 474
Email: dgali@mia.go.ug
Website: www.mia.go.ug

In any Correspondence on
this subject please
quote No.....

DFD 062/2025



MINISTRY OF INTERNAL AFFAIRS
DIRECTORATE OF GOVERNMENT
ANALYTICAL LABORATORY
Plot No. 2 Lourdel Road
Wandegeya,
P.O. Box 105639
Kampala - Uganda

18th March 2025

MR. KAYONGO RICHARD JEREMIAH AND MS SSEBAGALA SANDRA
REG NO. S21B32/129 & S19B32/663
UGANDA CHRISTIAN UNIVERSITY
P.O BOX 4,
MUKONO-UGANDA
Tel: 256-778-051449

REPORT OF ANALYSIS

Description of the Samples

Three samples of water were received from Mr. Kayongo Richard Jeremiah, on 13th March 2025 and was analysed from 14th to 18th March 2025. A summary of the sample received is shown in table below.

S/N	Description	Quantity	Assigned Lab ID
1	Filtrate water samples (03) packed in plastic bottles from the optimum mass column test	03	Samples "F1, F2, & F3" DFD 062/2025

Analysis Requested

To determine the Iron and Copper contents.

Method of Analysis

Analysis of Iron and Copper were analysed using AAS method.

Results of Analysis

The results are summarized in the table below:

Test/Parameter	Units	Results for DFD 062/2025			US EAS 12:2014
		Sample "F1"	Sample "F2"	Sample "F3"	
Copper (Cu)	mg/L	0.710	0.321	0.301	1.0 Max
Iron (Fe)	mg/L	0.617	0.234	0.212	0.3 Max

Remarks

1. The samples "F1, F2, & F3" DFD 062/2025 were analysed and found to comply with the limit of metals specified in the Ugandan standard for US EAS 12:2014, Potable water — Specification except Samples F1."
2. Results relate to sample analyzed and are reported as on received basis.

Fred - 18/3/25

Semalago Fredrick
Government Analyst

Telephone
+256 (0) 414 250 464 (Gen)
+256 (0) 414 250 474
Email: dgal@mia.go.ug
Website: www.mia.go.ug

In any Correspondence on
this subject please
quote No.....



DFD 063/2025

MINISTRY OF INTERNAL AFFAIRS
DIRECTORATE OF GOVERNMENT
ANALYTICAL LABORATORY
Plot No. 2 Lourdel Road
Wandegeya,
P.O. Box 105639
Kampala - Uganda

19th March 2025

MR. KAYONGO RICHARD JEREMIAH AND MS SSEBAGALA SANDRA
REG NO. S21B32/129 & S19B32/663.
UGANDA CHRISTIAN UNIVERSITY
P.O BOX 4,
MUKONO-UGANDA
Tel: 256-778-051449

REPORT OF ANALYSIS

Description of the Samples

Three samples of water were received from Mr. Kayongo Richard Jeremiah, on 17th March 2025 and was analysed from 17th to 19th March 2025. A summary of the sample received is shown in table below.

S/N	Description	Quantity	Assigned Lab ID
1	Filtrate water samples (06) packed in plastic bottles from the breakthrough curve column test	06	Samples "G1, G2, G3, G4, G5 & G6" DFD 063/2025

Analysis Requested

To determine the Iron and Copper contents.

Method of Analysis

Analysis of Iron and Copper were analysed using AAS method.

Results of Analysis

The results are summarized in the table below:

Test/ Parameter	Units	Results for DFD 063/2025						US EAS 12:2014
		Sample "G1"	Sample "G2"	Sample "G3"	Sample "G4"	Sample "G5"	Sample "G6"	
Copper (Cu)	mg/L	0.284	0.327	0.520	1.045	2.675	2.915	1.0 Max
Iron (Fe)	mg/L	0.204	0.256	0.685	1.505	2.805	2.940	0.3 Max

Remarks

1. The samples "G1, G2, G3, G4, G5 & G6" DFD 063/2025 were analysed and found to comply with the limit of metals specified in the Ugandan standard for US EAS 12:2014, Potable water — Specification except Samples G4, G5 & G6"
2. Results relate to sample analyzed and are reported as on received basis.

T

S. Fred 19/03/25

Semalago Fredrick
Government Analyst

"Go Scientific for a Safe and Just Society"

Page 1 of 1